A PRIVILEGED HUNTER:
ROLE OF NLRP7 IN IMMUNE PRIVILEGE

by

Duygu Demiröz

B.S., Molecular Biology and Genetics, Boğaziçi University, 2009

Submitted to the Institute for Graduate Studies in
Science and Engineering in partial fulfillment of
the requirements for the degree of
Master of Science

Graduate Program in Molecular Biology and Genetics
Boğaziçi University
2012

ACKNOWLEDGEMENTS

I would like to thank my supervisor Assoc. Prof. Nesrin Özören and my thesis committee members Assoc. Prof. Arzu Çelik and Asst. Prof. Ayça Sayı Yazgan for devoting their precious time to evaluate my thesis.

I am grateful to my boyfriend Levent Baş for standing always by me not only during hard times but also times of brainstorming and relieving the psychological pain of thesis writing and helping me with every small detail of it and drawing the figures in my thesis defense presentation with an admirable patience. Besides, I would like to thank my former project partner, one of my best friends Yetiş Gültekin for teaching me many of the techniques I know and for his support. I am also thankful to my current project partner Aybüke Alıcı Garipcan for her endless support, especially in imaginary NLRP7 projects.

I also want to express my thanks to Elif Eren for her help and support. Besides, I would like to express my appreciation to Serkan Uğurlu for helping me with the techniques. Also thanks go to my former and current labmates Burcu Sümer, Metehan Çifdalöz, Chara Charsou, Ali Can Sahillioğlu and Mustafa Yalçınkaya.

Special thanks to Ece Terzioğlu Kara, Çağrı Çevrim, Arzu Arat, Arzu Öztürk, Mustafa Talay, Duygu Koldere, Mustafa Can Ayhan, Zeynep Özcan, Bahar Şahin, Xalit Bayramlı, Aslı Uğurlu and Neslihan Zöhrap for being my friends and all the previous and current ACSF lab members for answering patiently my endless questions, especially during cloning experiments.

Additionally, I would like to thank to Prof. Cezmi Akdiş and Prof. Mübeccel Akdiş and all SIAF members both for supporting the work done in SIAF and making life

easier when living abroad. I also want to thank Cemalettin Bekpen for teaching me bio-informatic analysis and Stefan Fuss for teaching me confocal analysis.

I also thank to Assoc. Prof. Batu Erman, Emre Deniz and Nazlı Keskin for sharing the endosome marker plasmids and the antibiotic puromycin.

I am also grateful to Merve Baş, Mehmet Baş, Uğur Arpalı and his family for their endless hospitality and also Alp Kara for making me laugh in very bad times.

Finally, I am indebted to my family for supporting me under all cicumstances and in every decision I have made.

ABSTRACT

A PRIVILEGED HUNTER:
ROLE OF NLRP7 IN IMMUNE PRIVILEGE

NOD-like receptors (NLRs) are a family of cytoplasmic receptors with members regulating apoptosis and inflammation. NLRP7 is a novel PYRIN domain containing NLR family member and its functions are still under investigation. NLRP7 is known to possess an oncogenic role in testicular seminomas and found to be overexpressed in certain cancers. Interestingly, in addition to some other tissues, NLRP7 is expressed in brain, testis and placenta which are immune privilege sites in the body. Furthermore, mutations in NLRP7 can cause recurrent hydatidiform moles leading to stillbirths and abortions. One study suggested that NLRP7 down-regulates IL-1β and hence it is thought that NLRP7 may have an immuno-suppressive function. The aim of this project is to clarify the possible role of NLRP7 in immune privilege and also in inflammation. As a first step to the project, NLRP7 cDNA was cloned into several tagged (FLAG-, HA-, pcDNA3-MYC, RFP and EGFP) mammalian expression vectors for confocal analysis for cellular localization and for detection of its interaction partners by co-immunoprecipitation. The effect of NLRP7 overexpression on NF-κB signaling regulation was measured by performing luciferase assay in HEK293FT cells. In order to elucidate, in order to elucidate the possible role of NLRP7 in immune privilege, shifts in death receptor and HLA expressions were measured using real-time PCR and FACS analysis, respectively, in stable NLRP7 knock-down HEC-1-A cell line. Confocal analysis of RFP or EGFP fused NLRP7 reveals that NLRP7 is a cytosolic protein with minor co-localization to mitochondria. Furthermore, confocal co-localization studies show clear overlap between NLRP7 and caspase-1 and/or ASC. We also found that NLRP7 forms an inflammasome that activates IL-1β through binding to ASC and Caspase-1. NLRP7 appears likely to regulate IL-1β expression. Finally, NLRP7 down-regulation decreases the expression of TRAIL-R3, TNF-R2 and TWEAK and also HLA A, B, C and increases Fas expression.

ÖZET

AYRICALIKLI AVCI:
NLRP7'NİN İMMÜN AYRICALIKTAKİ ROLÜ

NOD-Benzeri-Alıcılar (NLR) üyeleri apoptoz ve enflamasyonu regüle eden sitoplazmik alıcılar ailesidir. NLRP7, PYRIN bölgesi içeren bir NLR üyesidir ve fonksiyonları henüz bilinmemektedir. NLRP7'nin testiküler seminomada onkogenik bir rol üstlendiği ve bazı kanser türlerinde fazlaca ifade edildiği yayınlanmış birkaç makalede gösterilmiştir. İlginçtir ki, NLRP7 beyin, testis ve plasenta gibi immün ayrıcalıklı dokular ile bazı başka dokularda ifade edilmektedir. Bunun yanında, NLRP7 mutasyonlarının kadınlarda ölü doğum ve düşüklerle sonuçlanan tekrarlayan hidatidiform mollere sebep olduğu bir çok farklı çalışmada gösterilmiştir. Ayrıca, NLRP7'nin IL-1β seviyelerini azalttığı ise bir makalede gösterilmiştir. Bu sebeple grubumuzca NLRP7'nin immün-baskılayıcı bir rolü olabileceği düşünülmüştür. Bu projenin amacı, NLRP7'nin immün ayrıcalıktaki ve enflamasyondaki olası rollerini belirlemektir. İlk olarak NLRP7 cDNA'sı konfokal hücresel lokalizasyon analizi ve immune-çöktürmeyle partner analizi için birçok vektöre klonlanmıştır (FLAG-, HA-, MYC-NLRP7 ve RFP-NLRP7, EGFP-NLRP7). Böylece NLRP7'nin HEK293FT hücrelerinde aşırı ifade edildiği koşullarda immün-çöktürme yöntemiyle etkileşim partnerleri ve lüsiferaz testiyle NF-κB yolağına olan etkileri belirlenmiştir. Bunlara ek olarak NLRP7'nin immün ayrıcalıktaki rolünü araştırmak için ölüm alıcıları ve HLA molekülleri ifadeleri, NLRP7'nin seviyelerinin stabil olarak düşürüldüğü HEC-1-A hücre hatlarında, gerçek zamanlı-PZR ve akış sitometrisi ile ölçülmüştür. RFP veya EGFP-NLRP7'nin hücresel lokalizasyonunun konfokal analizi sonucuna NLRP7'nin mitokondri ile minör ko-lokalizasyonu gözlemlenirken Kaspaz-1 ve/veya ASC'la çok net bir ko-lokalizasyon görülmüştür. Sonuçta, grubumuzca NLRP7'nin ASC ve Kaspaz-1'e bağlanarak bir inflamazom oluşturduğu ve IL-1β'yı olgunlaştırdığı ve ayrıca IL-1β'nın ekspresyonunu da regüle ettiği bulunmuştur. Ayrıca NLRP7 ifadesinin düşürülmesi sonucu TRAIL-R3, TNF-R2 ve TWEAK ve de ayrıca HLA A, B, C seviyeleri düşerken, Fas ifadesi artmıştır.

TABLE OF CONTENTS

LIST OF FIGURES

LIST OF TABLES

LIST OF SYMBOLS

bp	Base Pairs
g	Gravity
gr	Gram
kb	Kilobase
kDa	Kilodalton
L	Liter
M	Molar
mA	Milliamper
mg	Milligram
min	Minute
ml	Milliliter
mm	Millimeter
mM	Millimolar
ng	Nanogram
^{o}C	Centigrade degree
sec	Second
V	Volt
µg	Microgram
µl	Microliter
α	Alpha
β	Beta
γ	Gamma
κ	Kappa

LIST OF ACRONYMS / ABBREVIATIONS

ACAID	Anterior Chamber-Associated Immune Deviation
AD	Acidic Transactivator Domain
APC	Antigen Presenting Cell
APS	Ammonium Persulfate
ASC	Apoptosis Associated Speck-Like Protein Containing CARD
BIR	Baculovirus Inhibitor Repeat
BS	Behçet's Syndrome
BSA	Bovine Serum Albumin
CAPS	Cryopyrinopathies
CARD	Caspase Recruitment Domain
Caspase	Cysteine-Aspartic Proteases
CATERPILLAR	CARD, Transcription Enhancer, R-Binding, Pyrin, Lots of LRR
CBB	Commassie Brilliant Blue
CD	Cluster of Differentiation
cDNA	Complementary DNA
CFP	Cyan Fluorescent Protein
CIITA	Class II Transactivator
CLR	C-type Lectin Receptors
CO2	Carbondioxide
DAMP	Danger-Associated-Molecular-Patterns
DC	Dendritic Cell
DD	Death Domain
DED	Death Effector Domain
DMEM	Dulbecco's Modified Eagle Medium
DMSO	Dimethyl Sulfoxide
DNA	Deoxyribonucleic Acid
dsDNA	Double Stranded DNA
dsRNA	Double Stranded RNA
E. coli	*Escherichia coli*

EDTA	Ethylenediaminetetraacetic Acid
EGFP	Enhanced Green Fluorescent Protein
ER	Endoplasmic Reticulum
FasL	Fas Ligand
FBS	Fetal Bovine Serum
FCAS	Familial Cold Autoinflammatory Syndrome
FDA	Food and Drug Administration
GFP	Green Fluorescent Protein
GWAS	Genome-Wide Association Study
H_2O	Water
HBS	HEPES Balanced Salt
HEK	Human Embryonic Kidney
HLA	Human Leukocyte Antigen
IAP	Inhibitor of Apoptosis Proteins
IDO	Indoleamine-2,3-dioxygenase
iE-DAP	γ-d-glutamyl-meso-diaminopimelic acid
IFN	Interferon
IgG	Immunoglobulin G
IL	Interleukin
IL1R	IL1 Receptor
IL-1β	Interleukin 1- beta
IP	Immunoprecipitation
IRAK	IL1R Kinase
LB	Luria-Bertani Broth
LPS	Lipopolysaccaride
LRR	Leucin Rich Repeat
MAPK	Mitogen-Activated Protein Kinase
MDP	Muramyl Dipeptide
$MgCl_2$	Magnesium Chloride
MHC	Major Histocompatibility Complex
miRNA	MicroRNA
mRNA	Messanger RNA
mt	Mutant

MWS	Muckle-Wells Syndrome
NACHT	Domain Present in NAIP, CIITA, HET-E, TP-1
NaCl	Sodium Chloride
NAD	NACHT-associated Domain
NAIP	Neuronal Apoptosis Inhibitor Proteins
NBD	Nucleotide Binding Domain
NEAA	Non-esential Amino acid
NF-κB	Nuclear Factor kappa B
NK	Natural Killer
NLR	NOD-Like Receptor
NLRP	NBD, LRR and PYD Containing Proteins
NOD	Nucleotide-Binding Oligomerization Domain
NOMID	Neonatal Onset Multisystem Inflammatory Disease
OD	Optic Density
ORF	Open Reading Frame
PAMP	Pathogen-Associated Molecular Pattern
PB	Pacific Blue
PBS	Phosphate Buffered Saline
PCR	Polymerase Chain Reaction
PE	Phycoerythrin
Pen/Strep	Penicillin/Streptomycin
PGN	Peptidoglycan
PRM	Pathogen Recognition Molecules
PRR	Pattern Recognition Receptor
PYD	PYRIN Domain
RBC	Red Blood Cell
RFP	Red Fluorescent Protein
RHM	Recurrent Hydatidiform Mole
RIG-I	Retinoic acid-Inducible Gene-I
RIP	Receptor Interacting Protein
RLR	RIG-I like Receptor
RPM	Rotations per Minute
RT-PCR	Reverse Transcriptase Polymerase Chain Reaction

SDS	Sodium Dedocyl Sulfate
SDS-PAGE	SDS- Polyacrylamide Gel Electrophoresis
shRNA	Short Hairpin RNA
siRNA	Small Interference RNA
TAE	Tris-Acetate-EDTA
TBS	Tris Buffered Saline
TBST	Tris Buffered Saline Tween
TEMED	N,N,N',N'-Tetramethylethane-1,2-diamine
TGF	Transforming Growth Factor
TIR domain	Toll/IL-1 Receptor Domain
TLR	Toll-Like Receptor
TNF	Tumor Necrosis Factor
TRAF	TNF Receptor Associated Factor
Tween	Polysorbate
v	Volume
w	Weight
WB	Western Blot
WT	Wild-Type

1. INTRODUCTION

1.1. Immune System

The life span of humans is on average 70 years, chimpanzees' 40 years, dogs' 12 years, *Drosophila melanogaster*'s 30 days etc. On the other hand, any kind of pathogenic organism has a much faster proliferation rate. For instance *Mycobacterium tuberculosis*, the causative agent of many types of tuberculosis divides once in 15-20 hours. Due to the relatively long life of the host, the infecting pathogen is able to proliferate till all the sources of the host are totally consumed. The immune system is required for an organism to survive in an environment where thousands of pathogens live. It has evolved to eliminate the infectants of the organism, which helps us to overcome the infecting pathogens most of the time.

The defense of the host occurs at two levels: at the level of innate immunity and at the level of adaptive immunity. The latter is activated by the former just in case that the innate immune system is not able to eliminate the pathogen itself. Therefore, in order for the host to achieve a successful immune response innate and adaptive immune systems need to cooperate.

1.2. Innate Immune System

The innate immune system is an evolutionarily conserved defense mechanism among multicellular organisms against various pathogenic organisms. It establishes a rapid immune response upon encounter with a pathogen. Though non-specific to each pathogen, it is specific for conserved PAMPs (Pathogen Associated Molecular Patterns). In the late 1800s Elie Metchnikoff discovered phagocytes in starfish, which made him the founder of innate immunity (Akira, 2009). In 1908 he received the Nobel Prize for Medicine together with Paul Ehrlich, who developed the 'Side Chain Theory' that ex-

plained exactly how antibodies function. Then in the late 1980s Charles A. Janeway suggested that a limited number of germline-encoded receptors (PRRs) were the main actors in the formation of specific immune responses against various microbial molecules (PAMPs). Upon invasion by the pathogen, innate immune cells (macrophages, neutrophils, monocytes, mast cells and dendritic cells) (Medzhitov, 2001), that are capable of engulfing and destroying a broad range of pathogens, become activated. On the other hand, target-specific immune responses are elicited by the adaptive immune system. However, developing an adaptive response takes longer time in comparison to the innate immune response. Subsequently, in case the innate immune system is not sufficient to overcome an infection, the adaptive immune system, and firstly the helper T cells, are activated by the dendritic cells. For this, the dendritic cell that engulfs the pathogen needs to be activated as well, that is TLRs on the surface of dendritic cells bind their ligands that are specific for many pathogens. This priming of the TLR causes activation of many intracellular signaling pathways resulting in inflammatory cytokine (IL-12, IL-6, TNF, etc…) secretion and co-stimulatory molecule (CD40, CD80, CD86) production on the dendritic cell. In addition to antigen presentation these are required for T cell activation as the dendritic cell reaches the regional lymph node, which eventually activates B and T lymphocytes for memory as well as pathogen-specific immune responses, thereby developing an adaptive immune response.

In 1989, Janeway proposed that recognition of PAMPs that are conserved among pathogens, is achieved by specific host PRRs of the innate immune system cells (Janeway, 1989). In addition to PAMPs, PRRs recognize DAMPs that are nonmicrobial endogenous danger signals (Chen *et al.*, 2009). These PRRs induce immune responses either by recruiting antimicrobial factors or through intracellular signaling events. This results in cytokine and chemokine secretion from the cell and starts the inflammatory process. Several mediators produced in the inflammatory site cause vasodilation, which is essential for the recruitment of macrophages, monocytes and neutrophils and fluid leakage. This ends up in the four features of edema: redness, heat, swelling and pain.

Triggering of the intracellular signaling pathways can be achieved by TLRs and NLRs (Inohara *et al.*, 2005a). TLRs are membrane-bound receptors sensing the microbi-

al components either in the lumen of intracellular vesicles or outside the cell. On the other hand, NLRs are cytoplasmic receptors detecting intracellular PAMPs. RLRs (RIG-I like Receptors) are also in the cytoplasm for viral RNA recognition and antiviral response induction through type I IFN production (Yoneyama and Fujita, 2008). Finally, CLRs (C-type Lectin Receptors) bind to bacterial and fungal components CLRs have been conserved among metazoan species.

Plants have very similar pathogen recognition systems. Pathogen recognition is mediated by disease resistance *(R)* genes that are abundant in plant genomes and trigger hypersensitivity response causing the death of the infected cells and recruit antimicrobial compounds (Hulbert *et al.*, 2001) and cause morphological changes such as cell wall structure shifts to isolate the infected area (Inohara *et al.*, 2005b). The R gene family expresses proteins including transmembrane proteins carrying LRR ectodomains resembling the mammalian TLRs and cytoplasmic NLR proteins with central NOD domains and carboxy-terminal LRR domains (Dangl and Jones, 2001).

1.2.1. Toll-Like-Receptors

Initially, innate immunity was thought to be non-specific in terms of target recognition. This notion changed after the discovery of Toll, that is responsible for *Drosophila* dorsoventral axis formation during embryonal development and has a role in antifungal responses in flies (Lemaitre *et al.*, 1996), making the Toll protein the founder of the Toll-Like Receptor family. Accumulating evidence has proven that the innate immune system is able to distinguish between self and pathogens. Later the human homologue of Toll, TLR4 was identified as a PRR on the cell membrane leading to cytokine secretion and eventual adaptive immune response activation (Medzhitov *et al.*, 1997). Although first identified in *Drosophila melanogaster*, TLRs are found to be conserved among species including mammals and humans and they are expressed in various immune cells including macrophages, dendritic cells (DCs), B cells, certain type of T cells and non-immune cells such as fibroblasts and epithelial cells (Akira *et al.*, 2006). TLR

expression is dynamically regulated in response to pathogen invasion, cytokines and environmental stress.

TLRs are type I transmembrane proteins (their N-terminus is targeted to the ER lumen during their synthesis) that mediate defense against various bacterial, fungal and viral pathogens. They can reside on the plasma membrane or endosomal or lysosomal membranes, hence TLRs are able to recognize PAMPs outside the cell or inside endosomes or lysosomes. Recognition of PAMPs, including LPS, peptidoglycan, double-stranded RNA, flagellin, DNA, etc (Chen *et al.*, 2009, Kawai and Akira, 2009) is achieved through the LRRs in ectodomains of the TLRs, whereas the signal is transmitted inside the cell by the cytosolic TIR (Toll/IL-1 receptor) domain of the receptor via adaptor proteins such as MyD88, TIRAP, TRIF and TRAM (Akira *et al.*, 2006, Kawai and Akira, 2009).

TLRs are highly conserved from *Caenorhabditis elegans* to mammals. Out of 13 TLRs discovered so far TLR1 to TLR9 are conserved among humans and mice, although TLR10 of mice is not functional due to a retroviral insertion and humans lost TLR11, TLR12 and TLR13 from their genomes (Kawai and Akira, 2009).

1.2.2. NOD-Like Receptors

NOD-like proteins are cytoplasmic receptors including members regulating apoptosis and pathogen recognition. NLR family is evolutionarily conserved such that many organisms from various species possess homologs of mammalian NLRs including kingdoms plantea and animalia such as zebrafish (Laing *et al.*, 2008), plant (Dangl and Jones, 2001) and sea urchin (Sodergren *et al.*, 2006). The NLR family has 22 members in humans and mice have at least 33 NLR genes (Figure 1.1). The NLRs have conserved tripartite structure: an N-terminal effector domain for homophilic protein-protein interactions (can be CARD, PYD, BIR or AD domains), a central NOD domain required for self-oligomerization in order for the signaling complex to be activated and C-terminal LRR domain for ligand recognition.

Due to lack of consistency in the nomenclature of the NLR family, there were many names for the same protein, until over 100 scientists reached a consensus in March 2008 to reduce the confusion in naming the proteins, which was later approved by the Human Genome Organization Gene Nomenclature Committee and the Mouse Genomic Nomenclature Committee. According to this report there are 4 subfamilies of NLR family: NLRA (NLR family Acidic domain containing), NLRB (NLR family BIR domain containing), NLRC (NLR family CARD domain containing), NLRP (NLR family PYRIN domain containing) and also NLRX (NLR family with no strong homology to N-terminal domain of any other NLR subfamily member) (Ting *et al.*, 2008). CARD and PYRIN domains are members of death-domain fold superfamily, in other words, they are found in proteins functioning during apoptotic and inflammatory signaling. PYD is homologous to CARD and it is required for the homophilic interaction of the protein with another protein carrying PYD. On the other hand BIR domain is found in IAPs and NAIPs.

Like TLRs, NLR genes are expressed in both immune and non-immune cells including epithelial and mesothelial cells. The function of NLRs, studied so far, is induction of inflammatory cytokine and chemokine production and secretion. Therefore TLR and NLR's downstream targets, such as NF-κB, MAPK and Caspase-1, coincide to a great extent (Chen *et al.*, 2009).

The best characterized NLR family members are NOD1 and NOD2. They both recognize peptides derived from degradation of the bacterial cell wall component peptidoglycan, iE-DAP (γ-d-glutamyl-meso-diaminopimelic acid) and MDP (muramyl dipeptide), respectively. Although TLR2 residing on the cell membrane can bind to peptidoglycan (PDG) stemmed from Gram positive bacteria and trigger a signaling cascade resulting in pro-inflammatory cytokine secretion (Schwandner *et al.*, 1999), it is not able to sense the PDG derived peptides that are NOD1 or NOD2 ligands. Whereas MDP is present in all bacterial cell walls, iE-DAP is expressed by mostly Gram negative bacteria and certain Gram positive bacteria (Girardin *et al.*, 2003a, Girardin *et al.*, 2003b, Girardin *et al.*, 2003c). In the case of pathogen escape from the TLR2 receptor on the cell surface, then making use of pathogen secretion systems and pore forming toxins

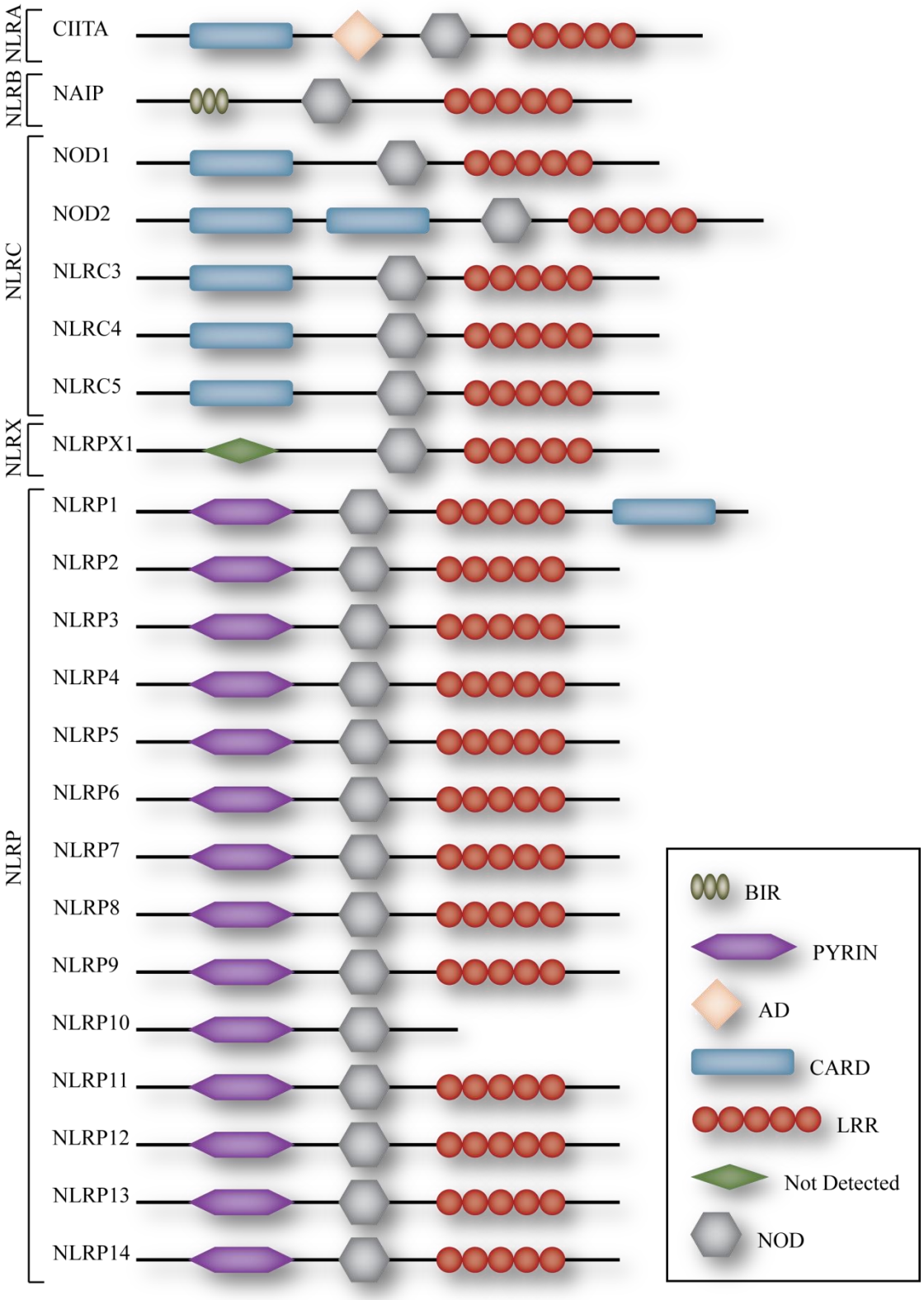

Figure 1.1. NOD like receptors.

(Ratner *et al.*, 2007), endocytosis and epithelial transporters such as PepT1 and PepT2, for MDP and iE-DAP, respectively (Ismair *et al.*, 2006, Swaan *et al.*, 2008), NOD1 and NOD2 can be activated. Upon ligand recognition they self-oligomerize and through action of various adaptor proteins including RICK, TAK1 and NEMO and in a ubiquitination-dependent manner they eventually activate the NF-κB transcription factor or MAPK, which activates transcription of several inflammatory cytokines and chemokines (Chen *et al.*, 2009). NLRs do not only activate NF-κB but certain members also suppress it. Thus far NLRP12 (Lich *et al.*, 2007), NLRC3 (Conti *et al.*, 2005), NLRP4 (Fiorentino *et al.*, 2002), NLRP10 (Wang *et al.*, 2004) and NLRP2 (Bruey *et al.*, 2004) were shown to inhibit NF-κB activity through either canonical or non-canonical ways. According to the paper published in 2005 by Kinoshita et al., NLRP7 (Kinoshita *et al.*, 2005), NLRP4 (Fiorentino *et al.*, 2002), NLRP10 (Wang *et al.*, 2004) and NLRP2 (Bruey *et al.*, 2004) form the anti-inflammatory subgroup although NLRP7 was shown to activate Caspase-1 by forming an ASC-dependent inflammasome, recently (Khare *et al.*, 2012).

1.2.3. Inflammasomes

In addition to their roles in NF-κB regulation, NLRs function in IL-1β production and secretion. For this purpose NLRP1, NLRP3 and NLRC4 (IPAF) can form inflammasomes i.e. multiprotein complexes that activate zymogens pro-caspase-1 and pro-caspase-5 by proximity-induced autocleavage. Among these three inflammasome-forming NLRs, NLRP1 and NLRC4 have CARD domains so they can directly bind to pro-caspase-1 and pro-caspase-5, whereas NLRP3 needs the adaptor ASC, consisting of both PYRIN and CARD domains. These activated caspases are utilized for cleavage of pro-IL-1β and pro-IL-18 into IL-1β and IL-18, the secreted forms, respectively (Figure 1.2). In addition to these, a non-NLR family member AIM2 can also form an inflammasome structure, employing ASC for recruitment and activation of Caspase-1 (Schroder and Tschopp, 2010).

Besides these, NLRs are found to have roles in organ homeostasis since several inflammatory and noninflammatory diseases are correlated with aberrant NLR signaling. For instance, gain of function mutations of NLRP3 cause MWS, FCAS and NOMID, and NOD2 gain of function mutations lead to Blau syndrome/early-onset sarcoidosis. On the other hand, loss of function mutations of NOD1 cause asthma and sarcoidosis and in case of CIITA function deficiency bare lymphocyte syndrome occurs (Chen *et al.*, 2009).

The NLR family has been discovered in the last decade and still there are many unknown aspects. The importance of NLRP gene products in the reproductive system is becoming more significant. For instance, deletion of NLRP5 in oocytes blocks embryo-

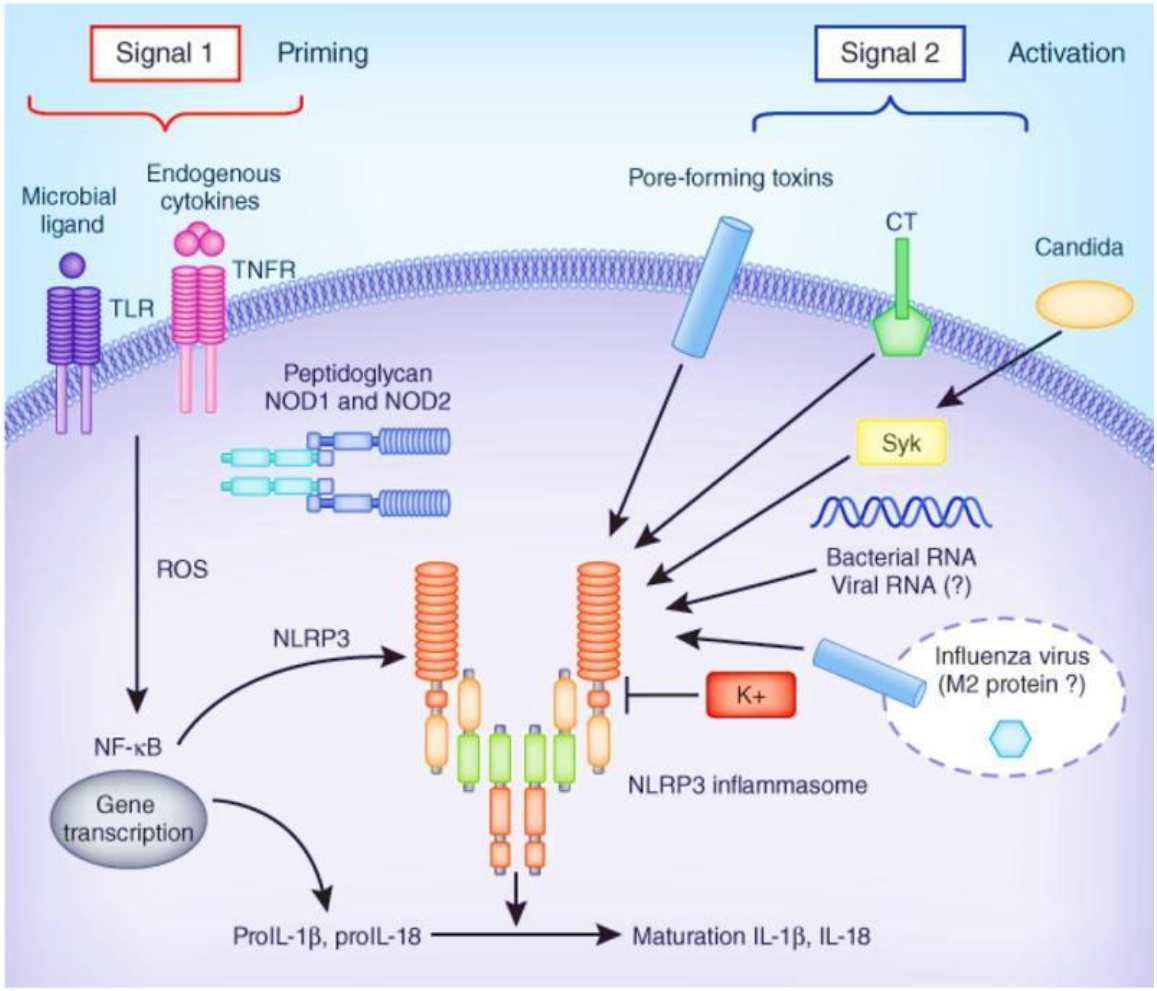

Figure 1.2. NLRs and NLRP3 inflammasome activation(Adapted from Franchi *et al.*, 2012)

nal development at the 2-cell stage resulting in female sterility in mice (Tong *et al.*, 2000). Also, when primordial (day 3) and primary (day 8) follicles of neonatal mice are compared, NLRP14 transcript levels are found to increase dramatically (Horikawa *et al.*, 2005). Another known reproduction-related-disease causing family member is NLRP7; mutations of NLRP7 cause recurrent hydatidiform moles, intrauterine growth retardation and abortions (Kou *et al.*, 2008, Qian *et al.*, 2007, Slim *et al.*, 2009, Slim and Mehio, 2007, Wang *et al.*, 2009).

1.3. NLRP7

NLRP7 is a less-well-studied member of NLRs with the first paper being published in 2005 where NLRP7 is proposed to have apoptosis and inflammation related functions. The human NLRP7 gene, located on locus 19q13.24, with gene length 23997 bp, encodes for the NLRP7 protein, which has three transcript variants produced as a result of alternative splicing. All three isoforms contain characteristic NLR family domains, namely PYD (pyrin domain), NACHT (domain present in NAIP, CIITA, HET-E, TP-1), NAD (NACHT-associated domain) and LRR (Leucin Rich Repeat) domains. Isoform 3 represents the longest transcript variant. Upon transcription isoform 1 is produced by splicing from an alternate site while isoform 2 lacks one exon, both resulting in shorter variants. Isoforms 1 and 3 have ten exons whereas isoform 2 has nine. In addition to humans, the NLRP7 gene is found in chimpanzee, rhesus macaque, orangutan, and marmoset, however it is not expressed in the mouse.

There are 23 mutations (Slim *et al.*, 2009) detected in locus 19q13.42 so far, all resulting in recurrent hydatidiform moles (RHM), a rare autosomal recessive disease caused by biparentally inherited DNA methylation (Kou *et al.*, 2008), leading to abortions. RHM mutations include NLRP7 gene splice site mutations, intragenic duplications and point mutations (Kou *et al.*, 2008, Qian *et al.*, 2007, Wang *et al.*, 2009).

Besides this reproduction-related-role, NLRP7 is suggested to have an oncogenic function since its expression increases in several testicular seminoma cell lines and pri-

mary human tissues in comparison with healthy controls (Okada *et al.*, 2004). NLRP7 has been shown to have a significant effect on the testicular tumor cell survival, however its overexpression has not been able to enhance tumor growth. Furthermore, NLRP7 expression has been reported to increase in endometrial cancer tissues and this increase correlated with myometrial invasion in human endometrial cancer and poor prognosis (Ohno *et al.*, 2008).

In 2005 NLRP7 was reported to suppress IL-1β secretion in a Caspase-1- dependent manner by inhibiting pro-caspase-1 and pro-IL-1β processing, without any effect on NF-κB activity (Kinoshita *et al.*, 2005). Also, in this study when THP1 cells and peripheral blood mononuclear cells were stimulated with LPS or IL-1β, this induced NLRP7 mRNA expression suggesting a negative feedback regulation of IL-1β secretion by NLRP7. Later, it was shown that, under *ex vivo* conditions, peripheral blood mononuclear cells from hydatidiform mole patients with NLRP7 mutations secrete less IL-1β in response to LPS in comparison to healthy control cells although they have increased pro-IL-1β synthesis. It was concluded that NLRP7 may have role in trafficking of IL-1β since it was found to be co-localized with microtubule organizing center and also with the Golgi (Messaed *et al.*, 2011).

1.4. Immune Privilege

In order to eradicate any infected cells and invading pathogens, the immune system has been organized in a very complex way. Regulation of this organization is even more crucial: the immune effector cells should be kept in check in the absence of an inflammation, during homeostasis state, and also during an inflammation event in order to prevent excessive tissue damage; otherwise survival of the organism can be endangered by the inflammatory response of the immune system. Besides, the immune system should be trained to be tolerant to self-antigens and also to commensal microorganisms in primary lymphoid organs and peripheral tissues (Barker and Billingham, 1977, Mellor and Munn, 2004). On the other hand, there are regions in the body that are privileged against inflammation. Immune privilege is a term used to characterize anatomical sites

where transplanted allografts have prolonged survival rates (Barker and Billingham, 1977). More generally it is a term used for the anatomical sites where active immune responses against both endogenous and exogenous antigens is suppressed by means of several strategies: 1) antigen sequestration behind certain barriers (blood-brain barrier, blood-testis barrier, blood-ocular barrier, trophoblast); 2) localized immunosuppression making use of certain cytokines and cell surface proteins; 3) lower lymphatic drainage (Meinhardt and Hedger, 2011).

The purpose of evolution is to continue life; therefore it would never allow the selection of a trait that aggravates the survival rate of the organism. Consequently, it is not surprising for a pregnant uterus, where the 'semiallogeneic' fetus faces with the maternal immune system, to be an immune privilege area. Otherwise, it would be inevitable to lose the embryos due to abortions, which in turn would be a catastrophe for the survival of the species. On the other hand, the testis, another important organ for evolution to proceed, is protected from most immune attacks by testicular immune privilege which is established during fetal development when the self-tolerance mechanisms are settled. Thus, in order to prevent attack on sperms or spermatocytes, so that the reproduction of the species is not endangered, immune system activity is suppressed at this site, which literally makes this area 'immune privileged'. Overall, immune privilege is an adaptation developed to protect the vital organs and tissues against inflammation. Otherwise these organs would not able to function properly, leading to the demise of the organism. Immune privilege areas include the brain, the cheek pouch of the hamster, hair follicles, testes, the pregnant uterus, the anterior chamber of the eye and the cornea (Niederkorn, 2006).

In the case of testicular immune privilege, the blood-testis barrier was thought to be the source of immune privilege due to its obstructive quality against the passage of immune cells, however, later it was shown that the interstitial fluid between the seminiferous tubules contains immune cells and has an efficient lymphatic drainage (Head *et al.*, 1983) . Besides, antibodies and lymphocytes against autoantigens of spermatogenic cells are found to be circulating freely in fertile men. Most importantly, immune privilege of the testis can be broken down upon introduction of activated lymphocytes of an

immunized donor to a naïve recipient or by immunization of the organism against testicular autoantigens. Thus, immune privilege in the testis is not a direct consequence of the blood-testis barrier, instead, other mechanisms are required for suppression of the immune system activity at this site (Meinhardt and Hedger, 2011). Clearly, the blood-testes barrier is not sufficient to establish and/or sustain the immune privileged status.

1.4.1. MHC Expression

MHC molecules are produced by almost every cell in the body in order to present the proteins synthesized in the cell to the immune system, so that the adaptive immune system detects the foreign molecules and activates the pathogen specific immune response. MHC Class I molecules are expressed by all nucleated cells whereas MHC Class II are specific to APCs, ie B cells, dendridic cells and macrophages.

In immune privilege areas of the body MHC expression on the cell surfaces has been determined to be decreased, leading to less antigen presentation to the immune system. Besides, there is a shift in the expression of classes of MHC molecules chosen for antigen presentation towards immunoregulatory types. For instance HLA-G and HLA-E rather than classical types of HLAs are expressed in the rhesus monkey testis and human spermatogenic cells (Fiszer *et al*., 1997, Ryan *et al.*, 2002).

1.4.2. Fas Ligand Expression

Fas is a TNF family member death receptor that resides on the cell surface and induces the extrinsic programmed cell death pathway upon ligand (FasL) binding. FasL is also a cell surface protein and thus, a cell that carries a FasL may lead to death of another cell carrying a Fas receptor. Fas is expressed on the surface of most cell types, on the other hand FasL is expressed only by NK and cytotoxic T cells. FasL-Fas receptor binding causes activation induced cell death and is a mechanism used by the cytotoxic T cells and NK cells for killing their target cell. On the other hand, this system is among

the strategies of immunosuppression applied in the immune privileged sites (Bellgrau *et al.*, 1995) and also for immune escape of many cancer cells including hepatocellular carcinoma, lymphoma, melanoma, astrocytoma, esophageal carcinoma, gastric adenocarcinoma, ovarian cancer, breast cancer etc... (Bennett *et al.*, 1999, Gao *et al.*, 1998, Gratas *et al.*, 1997, Igney and Krammer, 2005, Minas *et al.*, 2007, O'Connell *et al.*, 1999) in order to dynamically delete the antigen specific T cells and prevent antigen specific adaptive immune response activation.

1.4.3. IDO Expression

IDO (Indolamine 2,3-dioxygenase) is a tryptophan degrading intracellular enzyme produced in certain subtypes of macrophages and dendritic cells and in many tumors, and it is found to be functional in suppression of T cells (Mellor and Munn, 2004). It is constitutively active in the feto-maternal interface expressed by extravillous trophoblast cells in humans (Honig *et al.*, 2004, Kudo *et al.*, 2004). It is found to act by tryptophan deprivation in the environment resulting in cell cycle arrest of the T cells which makes these T cells more sensitized to apoptosis (Lee *et al.*, 2002, Munn *et al.*, 1999). It has been also shown that IDO metabolites are toxic to T cells (Fallarino *et al.*, 2002).

1.4.4. 'Immune Privilege Area-Associated' Immune Deviation

In addition to the above mentioned strategies, even if T cells are exposed to the environment in an immune privilege area, this leads to tolerance rather than attack. This notion originated from J.W. Streilein, to describe anterior chamber-associated immune deviation (ACAID). He found that upon injection of antigenic materials into the anterior chamber of the eye, deviant immune responses emerge (Mizuno *et al.*, 1989). This finding was later reproduced with several other allogeneic and histoincompatible tumor cells (Niederkorn *et al.*, 1983) and herpes simplex virus type I (Whittum *et al.*, 1982) injected into the anterior chamber of the eye and, another immune privilege area, testis (Ditzian-Kadanoff, 1999). Causing suppression of T cells against the tested antigens by injecting soluble antigens to these sites is generally called acquired immune deviation. Further-

more, it has been shown that upon transplantation of pancreatic islet cells into the mouse testis, memory cells were induced to die and numbers of regulatory T cells were found to be higher in comparison to conventional sites (Nasr *et al.*, 2005). These explain the tolerogenic environment of the immune privilege areas in an antigen specific manner.

Last but not least, there are cells in these tissues that permanently secrete cytokines with an immunosuppressive effect such as TGFβ secreting Sertoli cells and IL-10 secreting resident macrophages in the testis (Meinhardt and Hedger, 2011).

2. PURPOSE

NLRP7 is a novel protein, whose function is still largely unknown, seems to have various roles in apoptosis and inflammation related pathways. Expression of NLRP7 increases in testicular seminomas (Okada et al. 2004). There is conflicting evidence about NLRP7's effect on IL-1β release. While it was found to suppress IL-1β secretion in a Caspase-1-dependent manner in stably transfected NLRP7 expressing THP-1 cell lines (Kinoshita *et al.*, 2005), macrophages expressing NLRP7 endogenously are found to form an ASC-dependent inflammasome upon bacterial acylated-lipoprotein treatment leading to IL-1β release (Khare *et al.*, 2012). In other words, seems to regulate pro-inflammatory cytokine secretion and testicular tumor cell survival. Interestingly, NLRP7 is expressed in the brain, testis and placenta which are among the known immune privilege areas of the body. Activation of NOD1, another NLR family member, signaling leads to preterm delivery *in vivo*, because of a shift in cytokine secretion. Besides, caspase-1 levels were found to be elevated in amniotic fluids of women with preterm deliveries due to inflammation. Thus, the cytokine profile is critical for proper implantation and development of the embryo. Therefore, NLRP7 may have a role in the establishment and/or maintenance of immune privilege.

The aim of this thesis is to clone NLRP7 and study its functions in cell culture in order to identify its subcellular localization, its interaction partners and to produce NLRP7 knock-down and overexpression lines using endometrial cancer cells. Further characterization of NLRP7's functions will be achieved by finding its downstream pathways.

3. MATERIALS

3.1. Cell Lines

3.1.1. Human Embryonic Kidney Cell Line (HEK293FT)

The HEK293FT cell line was kindly provided by Prof. Maria Soengas from the Spanish National Cancer Research Center (CNIO, Madrid, Spain) and it is grown in DMEM supplemented with 10% FBS, 2mM L-Glutamine, 1x MEM Non-Essential Aminoacids, 100 U/ml penicilin and 100 µg/ml streptomycin.

3.1.2. HEC-1-A Cell Line

The HEC-1-A endometrial cancer cell line was purchased from the American Type Culture Collection, Virginia, USA and grown in McCoy's 5a Medium Modified supplemented with 10% FBS, 2 mM L-Glutamine, 1x MEM Non-Essential Aminoacids, 100 U/ml penicilin and 100 µg/ml streptomycin.

3.2. Chemicals, Plastic and Glassware

Chemicals were purchased from either Sigma (USA), Merck (Germany) or AppliChem (Germany). Plasticware from TPP (Switzerland) was preferred during cell culture studies whereas all the microcentrifuge tubes and tips were from Axygen (USA). All the glassware was autoclaved at 121^{o}C for 20 minutes for sterilization prior to use.

3.3. Buffers and Solutions

3.3.1. Cell Culture

Table 3.1. Solutions and media used in cell culture.

0.5% Trypsin-EDTA 10X	GibcoBRL, USA
DMSO	AppliChem, Germany
Dulbecco's Modified Eagle Medium (DMEM)	GibcoBRL, USA
Fetal Bovine Serum (FBS)	GibcoBRL, USA
McCoy's 5A Modified Medium	GibcoBRL, USA
MEM Non-essential amino acid (NEAA) 100X	GibcoBRL, USA
Penicillin/Streptomycin 100X (5000 u Penicillin + 5000 µg Streptomycin per ml)	GibcoBRL, USA

Table 3.2. Buffers used in cell culture.

Freezing Medium	20% FBS 1X Pen/Strep 100 µM MEM-NEAA 7.5% DMSO
MACS buffer	0.5% BSA 2 mM EDTA pH 7.4 in PBS
PBS 10X	80 gr NaCl 2 gr KCl 2.4 gr KH_2PO_4 14.4 gr Na_2HPO_4 Add ddH_2O upto 1 lt (pH 7.2)

3.3.2. Cloning and Analytic Digestion

Table 3.3. Enzymes used for cloning.

Restriction Enzymes	NEB, England
T4 DNA Ligase	NEB, England

3.3.3. Agarose Gel Electrophoresis

Table 3.4. Buffers and solutions used for agarose gel electrophoresis.

50X Tris Acetic acid EDTA (TAE)	2 M Tris-acetate 50 mM EDTA pH 8.5
DNA Ladder	DNA Ladder Mix Fermentas, Canada
Ethidium Bromide (EtBr)	Merck
Loading Dye	6x Loading Dye Fermentas, Canada

3.3.4. Transformation

Table 3.5. Antibiotics used for transformation.

Ampicillin	AppliChem, Germany
Kanamycin	Sigma, USA

Table 3.6. Media used for transformation.

LB Agar	1 L LB medium 15 gr Agar
LB Medium (1 L)	10 gr Tryptone 5 gr Yeast Extract 5 gr NaCl

3.3.5. Transfection

Table 3.7. Buffers and solutions used in transfection.

2X HBS Buffer	50 mM HEPES pH 7.0 280 mM NaCl 1.5 mM Na_2HPO_4
Chloroquine	AppliChem, Germany
HEPES	GibcoBRL, USA

3.3.6. Protein Isolation

Table 3.8. Buffers used for protein isolation.

Cell Lysis Buffer	1% Triton X 150 mM NaCl 20 mM Tris-HCl pH7.5 2 mM EDTA
Protease Inhibitor Cocktail	Roche, Germany

3.3.7. Western Blotting

Table 3.9. Buffers, solutions and supplements used for Western blotting.

Acrylamide:Bisacrylamide	29.2 gr Acrylamide 0.8 gr bisacryalmide In 100 ml
Ammonium Persulfate	10% APS (w/v)
Blocking Solution	5% non-fat milk in TBST
Coomassie Blue Staining Solution	0.1% Coomassie Blue 10% Acetic acid 50% Methanol in ddH_2O
Coomassie Blue Destaining Solution	10% Acetic acid 40% Methanol in ddH_2O
Ponceau Staining Solution	1 gr Ponceau 50 ml Acetic acid in 1L
Protein Ladders	PageRuler Prestained (SM0671) Fermentas PageRuler Prestained (26616) Thermo
15% Resolving Gel Stock	50 ml 30% Acrylamide 1 ml 10% SDS 20 ml 1.875M Tris 8.8 29 ml ddH_2O

Table 3.9. Buffers, solutions and supplements used for Western blotting (cont.).

15% Resolving for mini gel	8 ml 15% Resolving gel 80 µl 10% APS 8 µl TEMED
Running Buffer	1X Tris-Glycine buffer 0.1% SDS
6X Laemmli Sample Buffer	1.2 gr SDS 0.9 gr DTT 6 mg BPB 4.7 ml Glycerol 1.2 ml Tris 0.5M (pH 6.8) 2.1 ml ddH_2O
4% Stacking Gel Stock	3.3 ml 30% Acrylamide 250 µl 10% SDS 6.3 ml 0.5 M Tris (pH 6.8) 15 ml ddH_2O
4% Stacking gel for mini gel	4 ml 4% Stacking gel 40 µl 10% APS 4 µl TEMED
10X TBS	90 gr NaCl 121.14 gr Tris base Add ddH_2O upto 1 L (pH 7.5)
TBS-TWEEN	1X TBS 0.1% TWEEN 20
Transfer Buffer	39 mM Glycine 48 mM Tris-Base 0.0625% SDS
10X Tris-Glycine Buffer	15 gr Tris-Base 72 gr Glycine in 0.5 L ddH_2O

Table 3.10. Solutions used for western blotting.

Lumi-Light Western Blotting Substrate	Roche, Germany
Non-Fat Dry Milk	BIO-RAD
SDS	AppliChem, Germany
TWEEN	CalbioChem, Canada

3.3.8. Co-Immunoprecipitation

Table 3.11. Buffers and solutions used for co-immunoprecipitation.

Isotonic Lysis Buffer	1% Triton X 50 mM NaCl 20 mM Tris HCl pH7.5 2 mM EDTA
Protease Inhibitor Cocktail	Roche, Germany
Protein A/G Agarose beads	Pierce, USA
Lysis Buffer	1% Triton X 150 mM NaCl 20 mM Tris HCl pH7.5 2 mM EDTA 1 PIC tablet per 10 ml added prior to use

3.4. Fine Chemicals

3.4.1. Plasmids

Table 3.12. Plasmids used in this study.

dsRED MTS	AKLAB (BU-MBG)
pcDNA3-HA	Nunez Lab (UMICH, Ann Arbor, MI, USA)
pcDNA3-HA-NOD1	Nunez Lab (UMICH, Ann Arbor, MI, USA)
pcDNA3-FLAG	Nunez Lab (UMICH, Ann Arbor, MI, USA)
pcDNA3-FLAG- Caspase-1	Nunez Lab (UMICH, Ann Arbor, MI, USA)
pcDNA3-FLAG-ASC	AKİL
pcDNA3-FLAG-Caspase-5	AKİL
pcDNA3-MYC	Nunez Lab (UMICH, Ann Arbor, MI, USA)
pcDNA3-ASC	AKİL
pCFP-Rab5	Erman Lab (SU, Gebze, Turkey)
pCFP-Rab9	Erman Lab (SU, Gebze, Turkey)
pCFP-Rab1	Erman Lab (SU, Gebze, Turkey)
pCR-BluntII-TOPO	ImaGenes, Germany
pEGFP-C3	Retina Lab (BU-MBG)
pECFP-C1-Caspase-1	AKİL
pLenti-Ef-1a-ASC	AKİL
pTag-RFP-T	Tsien Lab (MIT, Boston, MA, USA)
shRNA 1-NLRP7	GeneCopoeia, USA
shRNA 2-NLRP7	GeneCopoeia, USA
shRNA 3-NLRP7	GeneCopoeia, USA
shRNA 4-NLRP7	GeneCopoeia, USA
scrambled-NLRP7	GeneCopoeia, USA

3.4.2. Primers

Table 3.13. Sequences of primers used in this study.

Primer Name	**Aim of Use**	**Sequence**	**Tm (C^o)**	**Introduced RE Cut-ting Site**
NLRP7_F	Cloning	TAGCTCTAGAACATCGCC CCAGCTAGAG	71.8	Xba I
NLRP7_R	Cloning	CCTAGCGGCCGCTCAGCA AAAAAAGTCACAGCA	76.6	Not I
NLRP7_Seq_F1	Sequencing	TGCAAGGAGCTCAGCCGC	60.8	-
NLRP7_Seq_F2	Sequencing	CTGAGCCTCCTGGCC	54.2	-
NLRP7_Seq_F3	Sequencing	GGTGCACTTACCTAACCA TTCCG	64.6	-
NLRP7_Seq_R	Sequencing	CGCTGATCCAGGACATCT	56.3	-
NLRP7_RT_F	Q-PCR	AGAGGCTGATGGCAAGAA ACT	59.5	-
NLRP7_RT_R	Q-PCR	TCTTGCACCTGTCCGTCCT	59.5	-
Ef-1a_F	Q-PCR	CTGAACCATCCAGGCCAA AT	58.4	-
Ef-1a_R	Q-PCR	GCCGTGTGGCAATCCAAT	56.3	-
Fas_F	Q-PCR	CTTTTCGTGAGCTCGTCT CTGA	62.1	-
Fas_R	Q-PCR	CCCCAGAAGCGTCTTTGA AC	60.5	-

Table 3.13. Sequences of primers used in this study (cont.).

FasL_F	Q-PCR	CCATTTAACAGGCAAGTC CAACT	60.9	-
FasL_R	Q-PCR	TCACTCCAGAAAGCAGGA CAATT	60.9	-
TRAIL_F	Q-PCR	CCCAATGACGAAGAGAGT ATGAACA	64.1	-
TRAIL_R	Q-PCR	CTCAAAATCATCTTTCTAA CGAGCTGA	63.7	-
TRAIL-R1_F	Q-PCR	TGTACGCCCTGGAGTGACAT	60.5	-
TRAIL-R1_R	Q-PCR	CACCAACAGCAACGGAACAA	58.4	-
TRAIL-R2_F	Q-PCR	CACTCACTGGAATGACCTC CTTT	62.9	-
TRAIL-R2_R	Q-PCR	GTGCAGGGACTTAGCTCCA CTT	64.2	-
TRAIL-R3_F	Q-PCR	CCCTAAAGTTCGTCGTCGT CAT	62.1	-
TRAIL-R3_R	Q-PCR	GGGCAGTGGTGGTGGCAG AGTA	67.9	-
TRAIL-R4_F	Q-PCR	ACAGAGGCGCAGCCTCAA	58.4	-
TRAIL-R4_R	Q-PCR	ACGGGTTACAGGCTCCAG TATATT	63.6	-
TWEAK_F	Q-PCR	CGCCTTTCCTGAACCGACTA	60.5	-
TWEAK_R	Q-PCR	CCGTGTTTTCCGGCCTT	54.9	-
TNF α_F	Q-PCR	CCAGGCAGTCAGATCATC TTCTC	64.6	-

Table 3.13. Sequences of primers used in this study (cont.).

TNF α_R	Q-PCR	GGAGCTGCCCCTCAGCTT	60.8	-
TNF-R1_F	Q-PCR	CGCTACCAACGGTGGAAG TC	62.5	-
TNF-R1_R	Q-PCR	TCCTTCAAGCTCCCCCTCTT	60.5	-
TNF-R2_F	Q-PCR	GAGTGGTGAACTGTGTCA TCATGA	63.6	-
TNF-R2_R	Q-PCR	GAGCTCGGCGCTGTGATC	60.8	-
TNFAIP_F	Q-PCR	GGGCGTTCAGGACACAGAC	61.6	-
TNFAIP_R	Q-PCR	CATCATTCCAGTTCCGAGT ATCA	60.9	-
OPG_F	Q-PCR	AAAGCACCCTGTAGAAAA CACA	58.4	-
OPG_R	Q-PCR	GTTGCCGTTTTATCCTCT CTAC	60.1	-
FN14_F	Q-PCR	GCTCTGAGCCTGACCTTC GT	62.5	-
FN14_R	Q-PCR	CTCTCCGCCGGTCTCCTC TA	64.6	-
p53_F	Q-PCR	TCAACAAGATGTTTTGCC AACTG	59.2	-
p53_R	Q-PCR	ATGTGCTGTGACTGCTTG TAGATG	59.2	-

3.4.3. Antibodies

Table 3.14. Antibodies used in this study.

Antibody	**Label**	**Host/Isotype**	**Company**	**Used Concen-tration**	**Aim**
HLA-E	APC	Mouse IgG1	eBioscience	0.25 µg for 10^6 cells	FACS
HLA-G	PE	Mouse IgG2a, κ	BioLegend	0.5 µg for 10^6 cells	FACS
HLA-A, B, C	PB	Mouse IgG2a, κ	BioLegend	0.5 µg for 10^6 cells	FACS
Mouse IgG1	APC	Mouse IgG1	eBioscience	0.25 µg for 10^6 cells	FACS
Mouse IgG2a, κ	PE	Mouse IgG2a, κ	BioLegend	0.5 µg for 10^6 cells	FACS
Mouse IgG2a, κ	PB	Mouse IgG2a, κ	BioLegend	0.5 µg for 10^6 cells	FACS
Caspase-1	-	Rabbit	Santa Cruz	1:200	WB
β-actin	-	Rabbit	Cell Signaling	1:1000	WB
FLAG	-	Rabbit	Cell Signaling	1:1000	WB
FLAG	-	Rabbit	Cell Signaling	1:200	CoIP
MYC	-	Rabbit	Cell Signaling	1:1000	WB
MYC	-	Rabbit	Cell Signaling	1:200	CoIP
ASC	-	Rabbit	Novus	1:1000	WB

Table 3.14. Antibodies used in this study.. Antibodies used in this study (cont.).

ASC	-	Mouse	Supernatant-Masumoto Lab (Shinshu U., Japan)	1:10	WB
Rabbit IgG	HRP	Gout	Cell Signaling	1:2000	WB
Mouse IgG	HRP	Rabbit	Cell Signaling	1:2000	WB

3.5. Kits

Table 3.15. Kits used in this study.

High Pure PCR Purification Kit	Roche, Germany
High Pure RNA Isolation Kit	Roche, Germany
High Pure Plasmid Isolation Kit	Roche, Germany
Genopure Plasmid Midi Kit	Roche, Germany
Genopure Plasmid Maxi Kit	Roche, Germany
Dual-Glo Luciferase Reporter Gene Assay	Promega, USA
ImPromII-Reverse Transcription System	Promega, USA
Revert Aid Reverse Transcription Kit	Fermentas, USA

3.6. Equipment

Table 3.16. Equipment used in this study.

Agarose Gel Electrophoresis	Agarose Gel System Thermo Scientific, USA
Agarose Gel Visualization System	Gel Doc XR System Bio Doc, Italy
Autoclaves	MAC 601, Eyela, Japan ASB260T, Astell, UK
Centrifuges	Allegra X22-R, Beckman, USA Himac CT4200C, Hitachi Koki, Japan J2-MC Centrifuge, Beckman, USA J2-21 Centrifuge, Beckman, USA
Freezers	2021D, Arçelik, Turkey 4250T, Arçelik, Turkey
Incubator	Hepa ClassII Forma Series, Thermo, USA
Heat Block	VWR, USA
Laminar Flow Cabinets	Class II A, Tezsan, Turkey Class II B, Tezsan, Turkey
Luminometer	Fluoraskan Ascent FL Thermo Scientific, USA
Magnetic Stirrer	Yellowline MSH Basic, USA
Microscopes	Zeiss, Axio Observer, Germany Z1 Inverted Mic., USA Leica, TCSSP5II, Germany Nikon, Eclipse TS100, Japan
Microwave oven	Arçelik, Turkey
pH meter	H221, Hanna Instr., USA
Pipettes	Gilson, USA

Table 3.16. Equipment used in this study.. Equipment used in this study (cont.).

Pipettors	Greiner-bio one, UK RatioLab acupetta, Germany
Power Supplies	EC135-90, Thermo Electron Corp Power Pac Universal, BIO-RAD, USA
PVDF Membrane Visualization	Stella, Raytest, Germany
Scales	Precisa XT4200C, Germany
SDS-PAGE Electrophoresis System	Mini-PROTEAN 4Cell, BIO-RAD, USA
SDS-PAGE Transfer System	Trans-Blot Semi-Dry BIO-RAD, USA
Shakers	Polymax 1010, USA Polymax 1040, USA Heildophl, Germany
Spectrophotometer	Nanodrop ND-100, Thermo, USA
Vortex	Fisons Whirli Mixer, UK GmcLab, Gilson, USA
Water Bath	GFL, Germany Memmert, Germany
Water filter	UTES, Turkey

4. METHODS

4.1. Cell Culture

4.1.1. Maintenance of HEK293FT Cell Lines

The HEK293FT human embryonic kidney cell line was kindly provided by Prof. Maria Soengas at Spanish National Cancer Research Centre Madrid, Spain. These cells were grown in DMEM supplemented with 10% FBS, 2mM L-Glutamine, 1x MEM Non-Essential Aminoacids, 100 U/ml penicilin and 100 µg/ml streptomycin. Cells were grown at 37^{o}C and 5% CO_2 incubator. Trypsin was used for subculturing. Freezing medium of the cells was 7% DMSO that was mixed with DMEM containing 20% FBS.

4.1.2. Maintenance of the HEC-1-A Cell Line

The HEC-1-A human uterus adenocarcinoma cell line was purchased from American Cell Culture Collection. These cells were grown in McCoy's 5a Medium Modified supplemented with 10% FBS, 2 mM L-Glutamine, 1x MEM Non-Essential Aminoacids, 100 U/ml penicilin and 100 µg/ml streptomycin. Cells were grown at 37^{o}C and 5% CO_2 incubator. The cells were washed with PBS containing 2mM EDTA and Trypsin-EDTA was used for subculturing. Freezing medium of the cells was 7% DMSO that was mixed with McCoy's 5a Medium Modified containing 20% FBS.

4.2. Cloning

4.2.1. Generation of pcDNA3-MYC-NLRP7

pcDNA3 vector was previously modified to insert FLAG, HA or MYC-tags just after the starting codon and in the 5' end of a gene that would be cloned into the vector (Nunez Lab, UMICH, Ann Arbor, MI, USA). Besides he original multiple cutting site of pcDNA3 was modified leading to different restriction enzyme cutting sites. In order to clone NLRP7 coding region into these vectors, first ORF of NLRP7 was found from NCBI database with the reference sequence NM_001127255.1. Upon analysis of the sequence using NEB Cutter V2.0 online tool for the restriction map, Xba I cutting site was added to the 5' end of the forward primer and Not I cutting site was added to the 5' end of the reverse primer. To increase the efficiency of the restriction enzyme cutting activity 4 additional nucleotides were added before the enzyme cutting sites in the primers.

The pCR-Blunt-II TOPO plasmid containing the NLRP7 cDNA was purchased from Imagenes. The region that encoded for NLRP7 cDNA was PCR amplified that introduced Xba I and Not I cutting sites to NLRP7 using 2 U Phusion DNA polymerase, Phusion High Fidelity Buffer, 0.4 µM from each primer, 0.6 mM dNTP and 3 mM $MgCl_2$. The PCR cycle was

Table 4.1. PCR cycle used for amplification of NLPP7 coding region.

98°C	1 minute	
98°C	10 seconds	26 cycles
59°C	40 seconds	
72°C	4 minutes	
72°C	1 minute	
4°C	∞	

2 µg of the PCR fragment was digested with 20 u Not I, and pcDNA3-MYC was digested with 40 U PspOM I at 37°C overnight. Before digesting with Xba I, the samples were purified using Roche High Pure PCR Product Purification Kit and Xba I digestion was performed with 30 U Xba I in buffer 4 at 37°C overnight. Then both vector and the insert were run on 1% agarose gel for 40 minutes at 125 V and both 5200 bp for the vector and 3300 bp for the insert were isolated from the gel using at Roche High Pure PCR Product Purification Kit.

4.2.2. Generation of pcDNA3-HA-NLRP7 and pcDNA3-FLAG-NLRP7

Since NLRP7 coding sequence had already been cloned into pcDNA3-MYC, only the tags were exchanged to get pcDNA3-HA-NLRP7 and pcDNA3-FLAG-NLRP7. For this purpose 1.6 µg from each of pcDNA3-MYC-NLRP7, pcDNA3-HA and pcDNA3-FLAG vectors was double digested with 20 U Xba I and 20 U Nde I with 100 µg/ml BSA in buffer 4 at 37°C overnight. Next day each sample was loaded on 1% agarose gel and run for 40 minutes at 125 V and 500 bp band from pcDNA3-HA and pcDNA3-FLAG digestion lanes and 8000 bp band from pcDNA3-MYC-NLRP7 were isolated using Roche High Pure PCR Product Purification Kit.

4.2.3. Generation of pEGFP-C3-NLRP7

2.5 µg pEGFP-C3-ASC vector was double digested with 20 U Sac I and 20 U Not I in buffer 4 with 100 µg/ml BSA in 30 µl at 37°C overnight. Also 11 µg Tag-RFP-T-NLRP7 vector was digested first with 100 U Not I in 100 µg/ml BSA in buffer 4 at 37°C overnight. Then since Sac I had an extra cutting site inside the vector, for partially digesting the Not I digested 11 µg Tag-RFP-T-NLRP7 vector, the digestion mixture of 87 µl was increased to 100 µl by the addition of 1.3 µl buffer 4, 100 µg/ml BSA and ddH_2O for partial digestion with Sac I. In another microcentrifuge tube 20 U of Sac I was diluted 1:10 in ddH_2O and 1 µl from this dilution was added to the reaction mix that was being incubated in 37°C at 0^{th}, 5^{th}, 15^{th} and 25^{th} minutes and reaction was stopped by heat inactivation of the restriction enzyme for 20 minutes at 80°C at the 30^{th} minute.

Then all the digestion product was run in 1% agarose gel at 120 V for 60 minutes in order for the isolation of 3300 bp band from the gel.

4.2.4. Generation of pLenti-Ef1a-RFP-NLRP7 Vector

2.4 µg Tag-RFP-T-NLRP7 vector was digested with 10 U Nhe I and 20 U Not I in 100 µg/ml BSA in buffer 4 at 37^{o}C overnight. Following purification of the band with Roche High Pure PCR Product Purification Kit, it was ligated with pLenti-Ef1a that had been digested with Nhe I and partially with Not I by A. Sahillioglu.

4.2.5. Generation of pLenti-Ef1a-EGFP-NLRP7 Vector

4 µg pEGFP-C3-NLRP7 vector was digested with 12 U Nhe I, 24 U NdeI and 24 U Not I in 100 µg/ml BSA in buffer 4 at 37^{o}C overnight. On the next day, the 4100 bp band was isolated upon run of the agarose gel since it had EGFP and NLRP7 fusion. Following purification of the band with Roche High Pure PCR Product Purification Kit, it was ligated with pLenti-Ef1a that had been digested with Nhe I and partially with Not I by A. Sahillioglu.

4.2.6. Generation of pET30a(+)-NLRP7

In order to clone NLRP7 into pET30a(+) vector which added His tag to the insert, NLRP7 was cut out from pEGFP-C3-NLRP7 clone using sequential digestion of Bgl II and Not I-HF. 1.5 µg from both pEGFP-C3-NLRP7 and pET30a(+) vector were digested with 10 U Bgl II overnight at 37^{o}C. After running the 1% agarose gel, 8300 bp band in pEGFP-C3-NLRP7 digestion lane and 5400 bp band in pET30a(+) lane were excised from the gel. The bands were purified followed by digestion with 10 U Not I-HF in buffer 4 for 90 minutes at 37^{o}C. Then another 1% agarose gel was run to excise the 3300 bp band from pEGFP-C3-NLRP7 lane and 5300 bp in pET30a(+) lane and purified using Roche High Pure PCR Product Purification Kit.

4.2.7. Ligation and Transformation into *E. coli*

Two digestion products were ligated in 3:1 insert to vector ratio resulting in 100 ng DNA in the final ligation reaction. Then 1.6 µl ligase buffer, 20 U T4 DNA ligase and ddH2O was added to get a final volume of 16 µl and the reaction was let to take place at 4^{o}C overnight.

The Top10 strain of *Escherichia coli* competent bacteria was let to melt on ice for 15 minutes and after addition of 8 µl from the ligation reaction, the bacteria-plasmid mix was incubated on ice for 10 minutes. Then the tube was transferred into 42^{o}C water bath for 90 seconds and the bacteria were heat shocked by transferring back to ice for 2 more minutes. Following addition of 500 µl LB without any antibiotics, the bacteria were let to grow on a shaker for at least 1 hour. At the end of 1 hour, the bacteria were spread onto agar plates with the antibiotic appropriate for the plasmid of interest.

Next four colonies on the plate were selected to grow in 6ml liquid LB medium with the appropriate antibiotic on shaker at 37^{o}C overnight and on the next day the plasmids were isolated using Roche High Pure Plasmid Isolation Kit and analytic digestion was performed with Eco RI restriction enzyme.

4.3. Agarose Gel Electrophoresis

1 gr agarose was added to 100 ml 1x TAE to obtain 1% agarose gel and this mixture was boiled in microwave oven until the agarose fully dissolved. After the mixture cooled down 30 ng/ml ethidium bromide was added and the gel was poured into a gel casting tray with the size depending on the purpose. After the gel solidified, it was placed in the agarose gel electrophoresis tank that was full of 1x TAE. Before loading the samples into the gel, each sample was mixed with 10x loading dye in 1:9 dye to sample ratio and the voltage and time of run varied depending on the size of the fragments.

4.4. Calcium Phosphate Transfection of HEK293FT Cells

The cells were seeded one day before transfection into plates differing in number depending on the purpose (Table 4.2) and incubated overnight at 37°C, 5% CO_2. On the day of transfection cells were treated with 25 μM chloroquine. Plasmid mix was prepared according to the aim and 250 mM calcium chloride ($CaCl_2$) and 2X HEPES Buffered Saline (HBS) solution were added on this plasmid mix dropwise. After 10 minute-incubation the DNA-$CaCl_2$ solution was added dropwise onto the previously chloroquine treated cells and the cells were incubated at 37°C, 5% CO_2 incubator. In order to remove chloroquine from the medium, after 6 hours media were replaced with fresh media. On the next day the expression of the co-transfected GFP or the fluorescent protein itself was observed to estimate the transfection efficiency.

Table 4.2. Number of cells seeded for each application.

Purpose	**Number of cells seeded per well**	**Plate**
Co-IP	$5*10^6$	10 cm
Virus Production	$2.8*10^6$	10 cm
Luciferase Assay	$8*10^5$	6-well
Cellular Localization Experiments	10^6	6-well
Viral transduction	$1.5*10^6$	6 cm

4.5. SDS-Polyacrylamide Gel Electrophoresis (PAGE) and Western Blotting

One day after transfection, the cells were harvested with Lysis Buffer and they were incubated on ice for 1 hour while vortexing periodically. Following 1 hour of lysis, the cells were centrifuged at 13000 RPM at +4°C for 30 minutes. At the end of centrifugation the supernatants were collected from each sample and to denature the proteins 6x Laemmli sample buffer was added to each sample followed by boiling at 95°C for 10minutes.

After pouring the 15% resolving and 5% stacking denaturing polyacrylamide gels (SDS-PAGE), respectively, with 1.5 mm thickness, the denatured samples were loaded and SDS-PAGE was run at 80 V and when the proteins entered the resolving gel, the voltage was increased to 120 V and running was continued till the BPB reached to the end of the gel.

Blotting papers (Sigma-Aldrich, USA) and PVDF membrane (Millipore, Ireland) were cut according to the size of the gel and semi-dry transfer for transferring the proteins to the PVDF-membrane was performed. For this purpose, blotting papers were wetted in cold transfer buffer whereas the membrane was activated by washing in methanol and excess methanol was removed with ddH_2O. Then both the membrane and the blotting papers were incubated in transfer buffer for 2-3min and placed on the semi-dry transfer apparatus in the following order from bottom to top: blotting paper, PVDF membrane, SDS-PAGE, blotting paper. And the transfer was performed at 100 mA for 90 min for each mini gel. After the transfer the membrane was blocked using 5% non-fat milk powder dissolved in TBST for 30 min and let to overnight incubation at 4^oC in the antibody solution (antibody of interest dissolved in blocking solution with a final dilution of 1:1000). On the next day unbound and non-specifically bound antibodies were removed by washing with TBST (3 x 5 min) and the membrane was incubated in secondary antibody solution (secondary antibody that was conjugated to HRP enzyme, 1:2000 diluted in blocking solution) for 2 hours at room temperature. Finally, after washing the membrane with TBST (3 x 5 min) to remove unbound and weakly bound antibodies, the substrate for HRP and required buffer (Lumi-Light Western Blotting Substrate (Roche, Germany)) were mixed 1:1 and 1 ml from this mixture was added onto the membrane to visualize the protein bands. After 5 minutes of incubation the bands were visualized in Stella and ‘very sensitive’ image program was selected to detect the proteins on the membrane. In order to check the presence of other proteins on the same membrane, the membrane was washed with TBST and incubated in new primary antibody solution overnight, as stated before, without stripping.

4.6. Co-Immunoprecipitation

Two days after transfection (Table 4.3), making sure the transfection efficiency was >80% of the HEK293FT cells with the interested plasmids, the cells were collected by trypsinization and washed with cold PBS 3 times. Then, using 500 µl 1% Triton X-100 lysis buffer, containing protease inhibitor cocktail, the cells were lysed for 1 hour incubation on ice while vortexing gently and periodically. This was followed by 30 minute-centrifugation at 13000 RPM at 4^{o}C. 400 µl of the supernatant was added onto 20 µl of Protein A/G Agarose beads, which were already washed 3 times with the lysis buffer while left 100µl of the supernatant was kept as whole cell lysate sample. The bead-supernatant mix was incubated on shaker at 4^{o}C for 30 minutes. At the end of this incubation, the tubes were centrifuged for 15 seconds at 13000 RPM at 4^{o}C for discarding the beads that bound to the proteins non-specifically. The supernatant was added onto fresh 50 µl of Protein A/G Agarose beads that was previously washed three times with the cold lysis buffer and 2 µl (1:200 dilution since starting amount was 400 µl) anti-FLAG antibody was added to this mixture and the tubes were incubated overnight at 4^{o}C.

Table 4.3. Co-immunoprecipitation plasmid mixes.

Plasmid	**Transfected Plasmid Amount (ng)**	
	Test	**Negative control**
FLAG-Caspase-1 or FLAG-Caspase-5 or FLAG-ASC	2000	-
MYC-NLRP7	7000	-
FLAG-empty	-	2000
MYC-empty	-	7000

On the next day, the beads bound by the antibody-protein complexes were washed three times with isotonic 1% Triton X-100 buffer in between 15 second cold centrifugations of 13000 RPM and eventually Western blotting was performed after suspension of the beads in 30 µl of isotonic 1% Triton X-100 buffer.

4.7. Confocal Analysis

The cells to be visualized were seeded on cover slips in six-well plates the day before transfection. One day after transfection, the cover slips were washed with 1x PBS, fixed with paraformaldehyde and the cells were visualized using Leica TCS SP5 II upright confocal microscope. RFP or dsRED, EGFP and ECFP were monitored by sequential scan and EGFP was excited by 488 nm, ECFP by 458 nm lasers. For quantification, photos from different areas were taken and the cells that seem to be alive were counted only. For the co-localization counts only the cells that were counted as positive.

4.8. Inflammasome Activation Assay

Two days after transfecting 10^6 HEK293FT cells in 6-well plates using the calcium phosphate method with 1 µg of each of the inflammasome components and pro-IL-1β depending on the purpose (Figure 5.18), intracellular mature IL-1β levels were measured by quantification of band intensities in Western Blot. In order to equalize the transfected DNA amount empty pcDNA3 plasmid was added to the plasmid mixes.

4.9. Production of NLRP7 Knock Down HEC-1-A Cell Line

Two days after transfecting $2.8*10^6$ HEK293FT cells in 10cm plates using the calcium phosphate method with the amounts shown in Table 4.2, the supernatants of the cells containing the viral particles were collected. In order to concentrate and change the DMEM medium to McCoy's 5A modified medium, the supernatant was centrifuged overnight at 18000 g at 4^oC. Then polybreen was added to the pellet, that was dissolved

in 2.5 ml McCoy's 5A modified medium, to a final concentration of 4 µg/ml and the mixture was filtered with 0.45 µM filters and added drop by drop onto $1.5*10^6$ HEC-1-A cells seeded the day before into 6 cm plates. 5 h after transduction the medium was replaced with the fresh medium. After 1 week with increasing expression of mCherry that was observed under fluorescent microscope, HEC-1-A cells that were stably expressing the shRNA were selected by treatment with 2 µg/ml puromycin.

Table 4.4. Lentivirus production plasmid mix.

Plasmid	**Amount (ng)**
pDelta	220
VSV- G	1800
shRNA or scrabled	2000

4.10. Real-Time Detection of Death Receptors and Certain Cytokines

After having the puromycin resistant HEC-1-A cell lines expressing shRNA1 and scrambled RNA, total RNA was isolated from each using Qiagen RNeasy Mini Kit according to supplier's suggestions. Then, in order to produce cDNA reverse transcription was performed using Fermentas Revert Aid reverse Transcriptase. For this 1500 ng total RNA was mixed with 0.2 µg random hexamer primer and RNase free ddH_2O upto 12.5 µl and this mixture was incubated for 5 minutes at 65^oC and 10 minutes at 4^oC. At the same time in another tube reaction master mix was prepared as:

Table 4.5. Master mix final concentrations for real time detection.

	Final Concentration
5x Reaction Buffer	1x
RiboLock RNase Inhibitor	20 U
dNTP mix	1 mM
Revert Aid Reverse Transcriptase	200 U

Before starting the RT-PCR reaction 7.5 µl from the reaction master mix was delivered to each reaction tube and reaction was performed as:

Table 4.6. Reaction conditions applied before RT-PCR.

25^{o}C	10 minutes
42^{o}C	60 minutes
70^{o}C	10 minutes

As the reaction completed, before performing the Real-Time PCR, the cDNA was diluted in 1:12.5 ratio with RNase free ddH_2O and 5 µl from this dilution was utilized for each reaction in Q-PCR and each reaction was performed in triplicates in 384-well plates. The reaction mix for each well contains:

Table 4.7. Q-PCR reaction mix.

SYBR Green Ready Mix	7.35 µl
Primer Mix (Forward and Reverse Primers)	1 µM from each primer
cDNA	5 µl
ddH_2O	
TOTAL VOLUME	9.7 µl

4.11. Cell Surface Staining

Parental HEC-1-A cells and lentivirally transduced scrambled and shRNA NLRP7 expressing lines were trypsinized and incubated overnight on the roller in the usual cell culture incubator to let the cells to express surface proteins where they could not attach to the surface. On the next day cells were centrifuged and the pellets were dissolved in cold MACS buffer so that the cell concentration would be $20*10^6$/ml. Then 50 µl (10^6 cells for each staining) from the cell suspension was put into special U-bottom flow cytometer tubes and primary antibodies and isotype controls for non-specific binding detection were added as shown in Table 4.8.

Table 4.8. Antibodies and corresponding isotype controls used in flow cytometry experiments.

Antibody	**Required amount**	**Required volume**	**Corresponding Isotype control**	**Required amount**	**Required volume**
PE-Fas	-	10 µl	PE-Mouse IgG1	-	5 µl
PE-FasL	1 µg	20 µl	PE-Mouse IgG2b	1 µg	40 µl
PE-TRAIL	0.06 µg	5 µl	PE-Mouse IgG1, κ	-	10 µl
PE-TRAIL-R1	1 µg	40 µl	PE-Mouse IgG1	-	5 µl
PE-TRAIL-R3	1 µg	40 µl	PE-Mouse IgG1	-	5 µl
PE-TNF-RII	0.25 µg	10 µl	PE-Mouse IgG2a	0.25 µg	25 µl
PE-TWEAK	-	20 µl	PE-Mouse IgG3, κ	-	-
PB-HLA A, B, C	0.5 µg	1 µl	PB-Mouse IgG2a, κ	0.5 µg	1 µl
APC-HLA E	0.5 µg	5 µl	APC-Mouse IgG1, κ	0.5 µg	20 µl
PE-HLA G	1 µg	20 µl	PE-Mouse IgG2a, κ	1 µg	5 µl

And each tube was filled upto 100 µl with the MACS buffer. Tubes were incubated for 30 minutes at 4^oC and washed twice with MACS buffer between centrifugations of 350 g for 7 minutes each. Finally, each sample was analyzed together with the isotype and compensation controls in Beckman Coulter Gallios^{TM} Flow Cytometer. First,

unstained parental lines were read since they had no fluorescence in order to set the gates. Next, for multiple stainings, as in the case of HLA stainings, each antibody's binding were read separately first from the tubes that contain individual antibodies for compensation settings and then the tubes with the triple staining were read. Also, the isotype controls were read to detect how nonspecifically bound the antibodies to their antigens. Finally, the data was analyzed using the program KALUZA 1.2.

4.12. Luciferase Reporter Gene Assay for NF-κB Activity Measurement

One day after transfection of the plasmid mixes (Table 4.9), NF-κB dependent transcription was measured with Dual-Glo Luciferase Assay System (Promega, USA). To normalize the measurements pRL-TK Luc renilla plasmid was co-transfected with pBVIx-Luc and assays were done in triplicates.

Table 4.9. Luciferase assay plasmid mixes.

	Negative control	**pcDNA3-MYC-NLRP7 gradient**				**NOD1 control**
		10 ng	**50 ng**	**100 ng**	**100 ng**	
pcDNA3-MYC-NLRP7	-	10	50	100	100	-
pEGFP-C3	64	64	64	64	64	64
pRL-TK- Luc renilla	5	5	5	5	5	5
pBVIx-Luc firefly	50	50	50	50	50	50
pcDNA3-HA-NOD1	-	100	100	100	-	100
empty pcDNA3	201	91	51	1	101	101

4.13. Phylogenetic Analysis

The phylogenetic tree was constructed with Mega 4.0 software using Neighbor-Joining method upon nucleotide sequence alignment with online ClustalW2 tool. All the positions with gaps or deletions were eliminated during the analysis. The bootstrap consensus tree was constructed from 1000 replicates.

5. RESULTS

5.1. Primary Structural Analysis of NLRP7 cDNA

The NLRP7 protein is composed of three domains: N-terminal effector domain, namely PYRIN, central NACHT domain and C-terminal LRR domain (Figure 5.1).

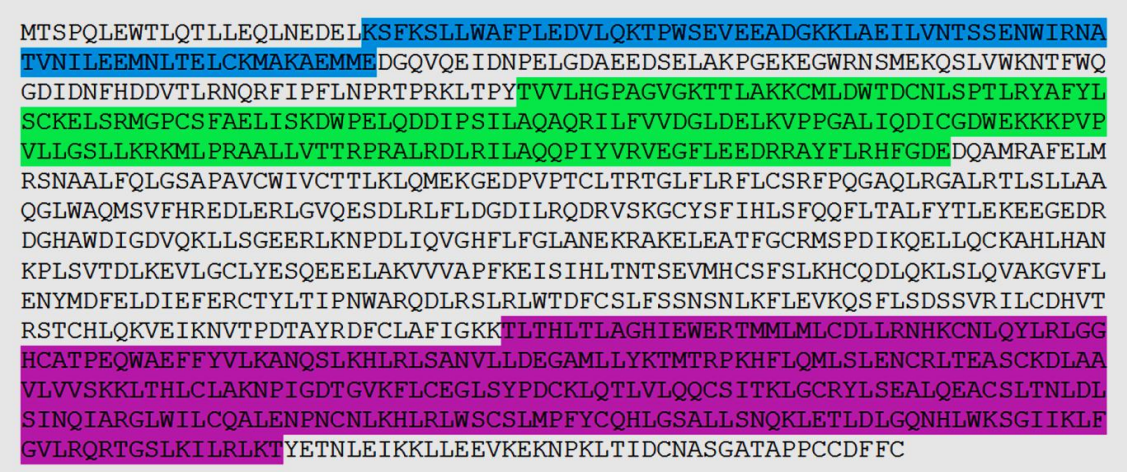

Figure 5.1. Domain organization of NLRP7. (Blue: PYRIN domain, Green: NACHT domain, Purple: LRR domain)

According to the NCBI Nucleotide database NLRP7 was found to be expressed only in primates among the organisms whose genomic sequences were fully available including human, rhesus monkey, marmoset, chimpanzee and orangutan (Figure 5.2). NLRP7 amino acid sequences were found to be highly conserved among these five species. Human NLRP7 protein sequence was calculated to be 95% identical to chimpanzee, 75% to orangutan, 88% to macaque and 76% to marmoset using GeneDoc 2.7.000 software. However, NLRP7 is not expressed in cow, dog and mice.

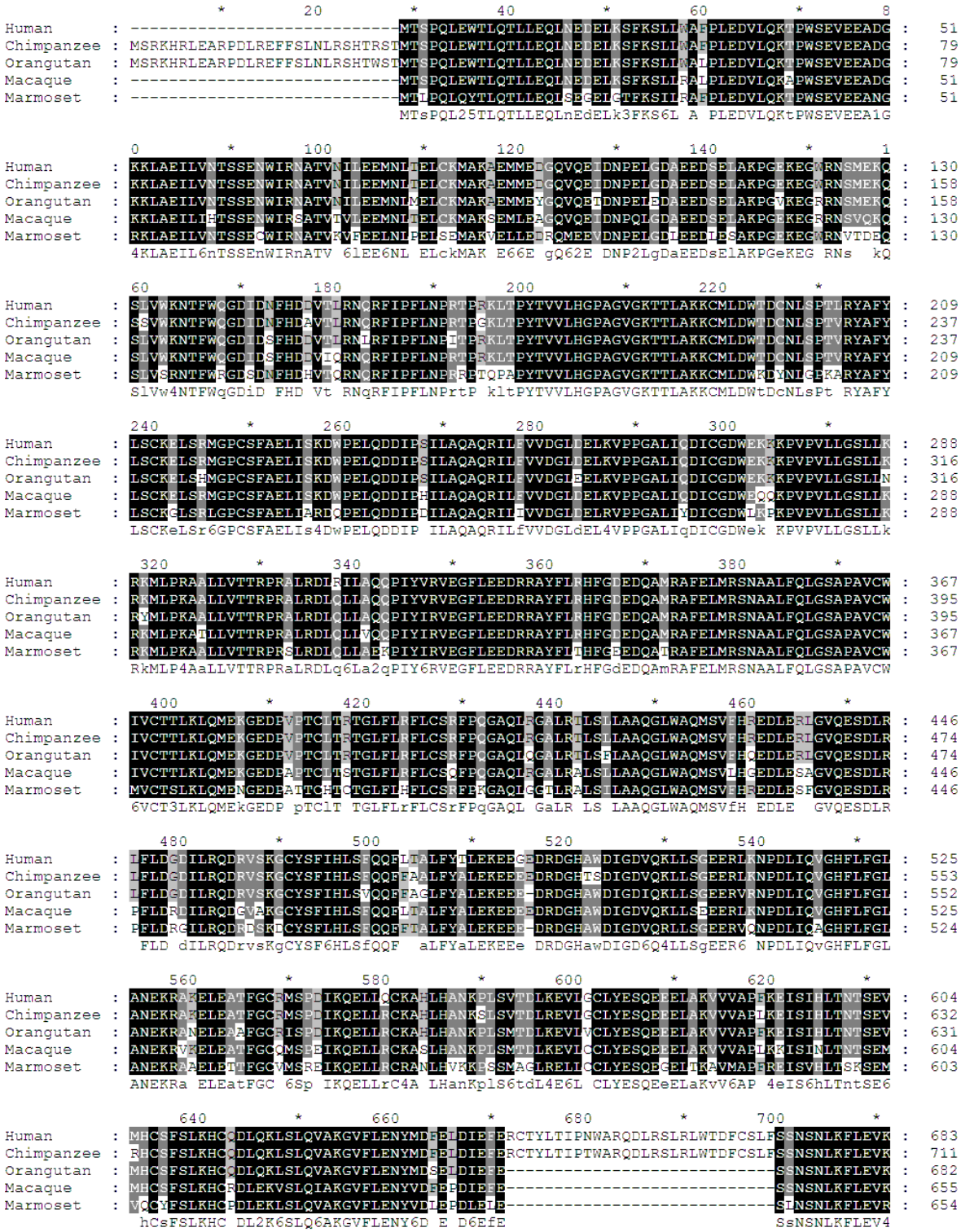

Figure 5.2. NLRP7 amino acid sequence alignment among primate species.

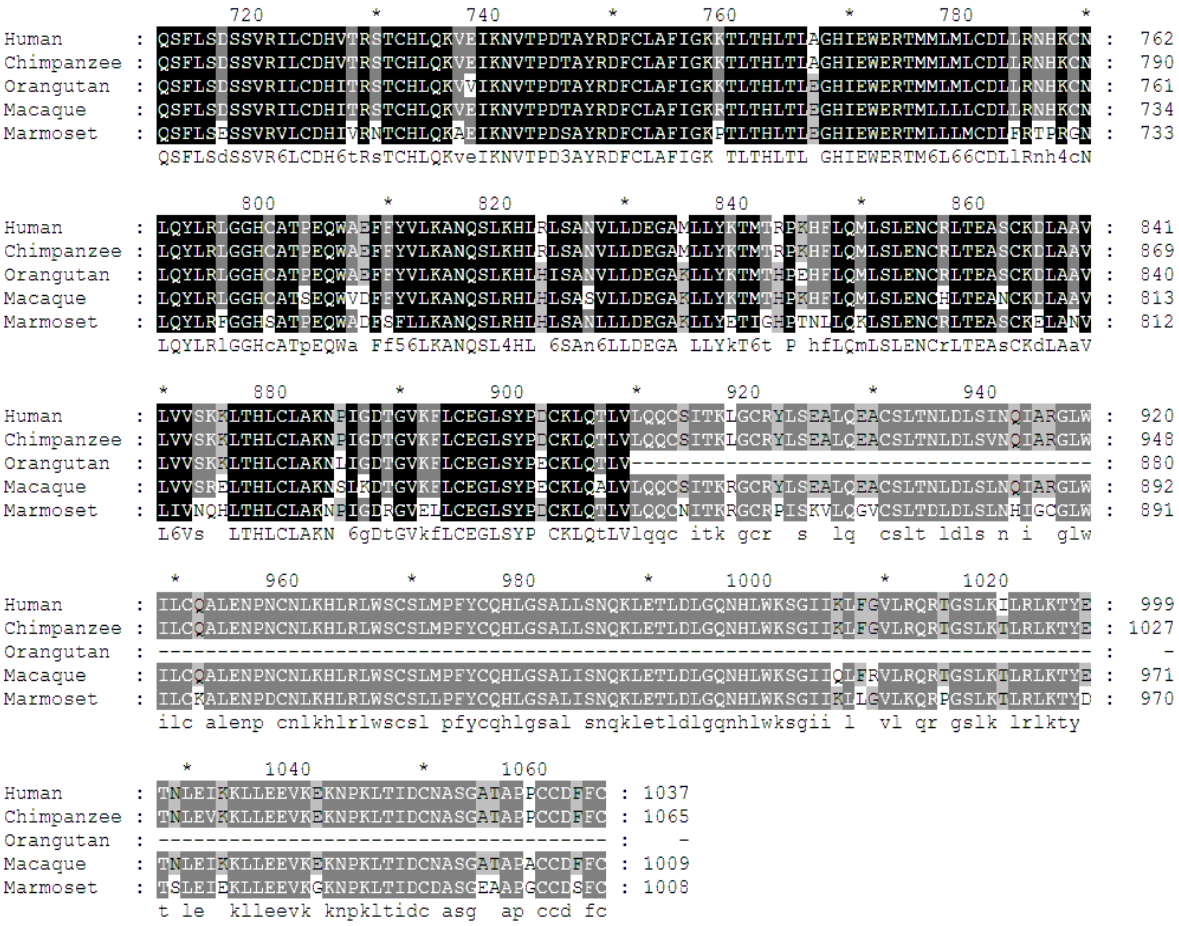

Figure 5.2. NLRP7 amino acid sequence alignment among primate species.. NLRP7 amino acid sequence alignment among primate species (cont.).

Besides, upon blasting NLRP7 nucleotide sequence against the whole human genome, it was found to have highest homology with NLRP2 which is expressed in many other organisms. Thus, NLRP2 was used as an outgroup in order to construct the phylogenetic tree of NLRP7 using their nucleotide sequences (Figure 5.3). It was concluded from these bioinformatic analysis that NLRP7 is a primate-specific gene with high aminoacid sequence conservation and it is closest relative is NLRP2 which is expressed in several more species.

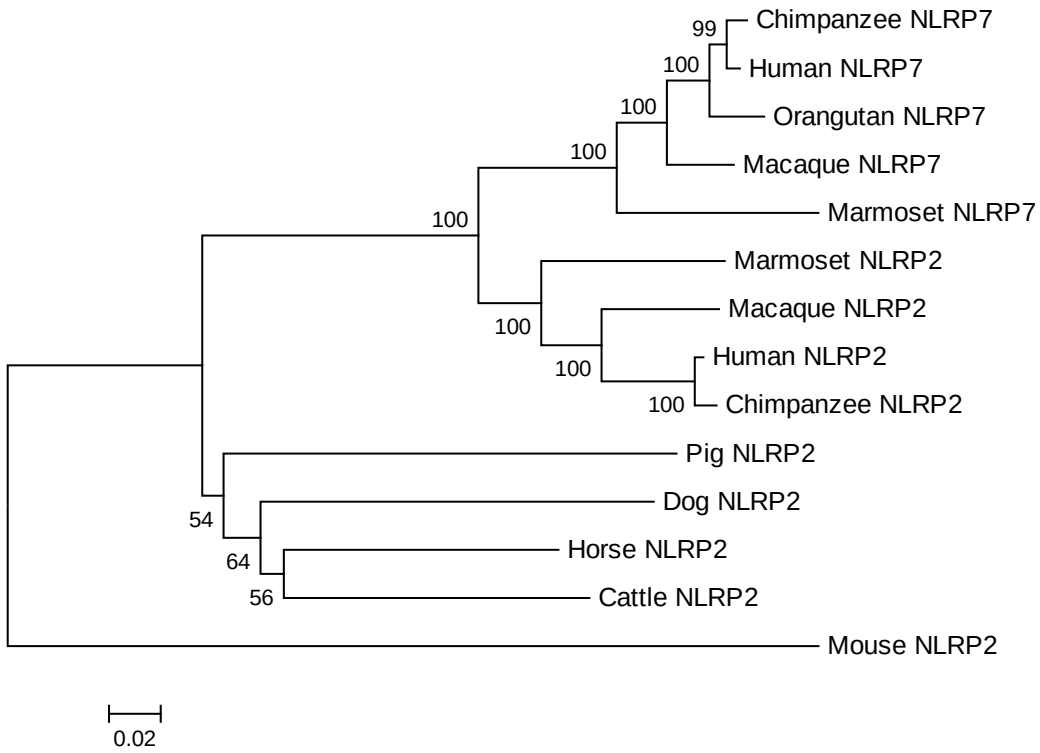

Figure 5.3. Phylogenetic analysis of NLRP7 among species using Neighbor-Joining method using Mega 4.0 software. All the positions with missing nucleotides were excluded from the dataset resulting in 1466 nucleotides in the final dataset.

5.2. Preparation of NLRP7 Mammalian Expression Constructs

In order to be used in functional experiments various expression constructs for NLRP7 were produced.

5.2.1. Production of pcDNA3-MYC-NLRP7 Construct

To be able to detect the NRP7 protein, tagged proteins were designed, such that the NLRP7 protein was tagged with HA, MYC and FLAG. pCR-Blunt_II-TOPO vector comprising NLRP7 cDNA was purchased from the ImaGenes GmbH. According to the DNA sequence obtained from NCBI Nucleotide Database gene specific primers were designed to have Xba I and Not I restriction enzyme cutting sites at the 5’ ends of the

forward and reverse primers, respectively. Using the purchased vector as a template gene specific PCR was performed in order to amplify NLRP7 cDNA with Finnzyme Phusion High Fidelity Taq Polymerase (Figure 5.4a). Then the PCR product was digested with Xba I and Not I and cloned into Xba I , PspOM I–digested pcDNA3-MYC vector Four colonies were analysed using restriction digestion with Nco I to detect the presence of NLRP7. Two colonies (colony 3 and 4) produced the expected restriction pattern (3900 bp, 3300 bp, 700 bp and 300 bp) (Figure 5.4b). Both colonies were sequenced and colony 3 was shown to be mutation-free.

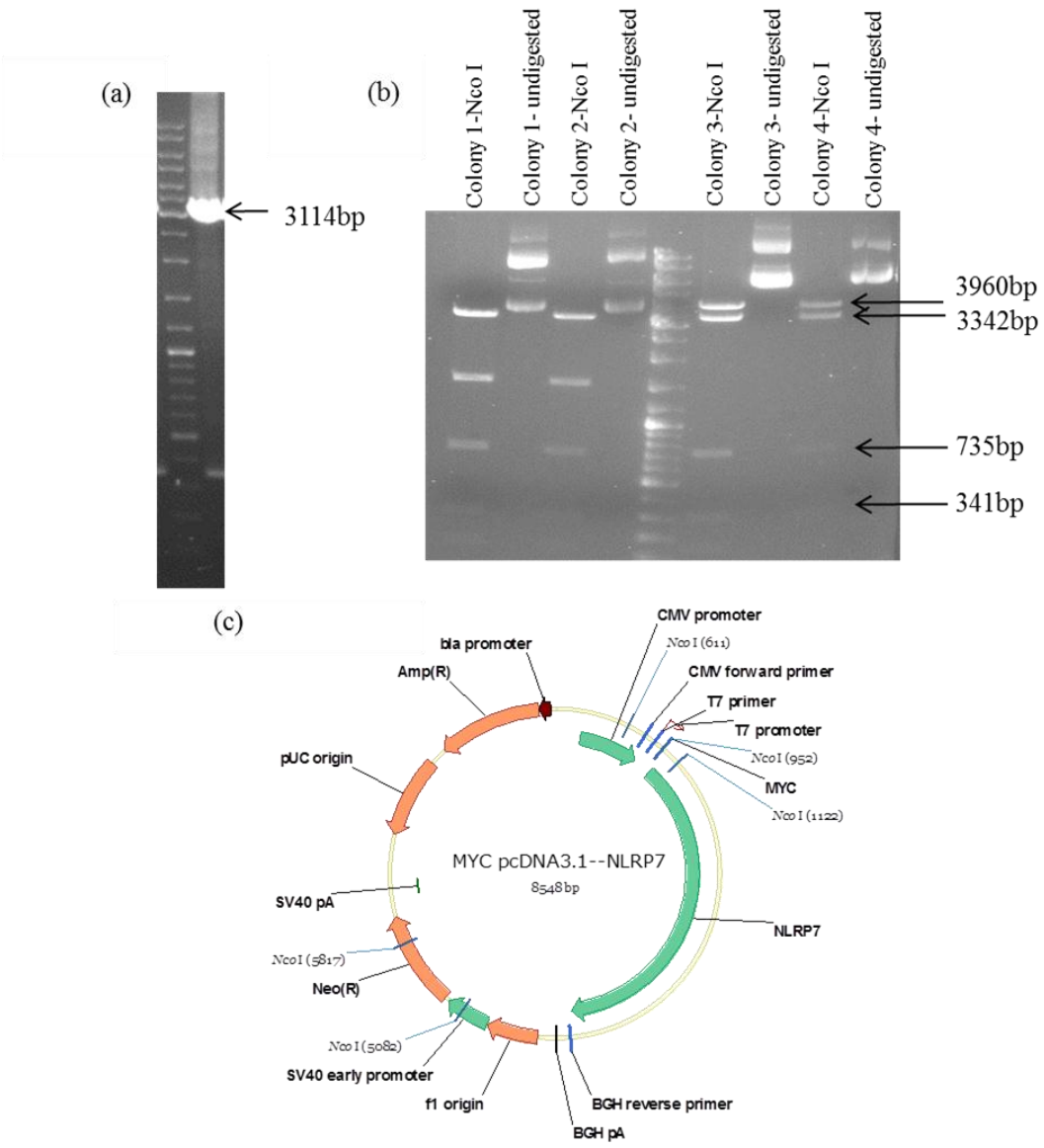

Figure 5.4. Cloning of NLRP7 into pcDNA3-MYC. (a) PCR amplification of NLRP7 (b) Analytic digestion of pcDNA3-MYC-NLRP7 (c) Map of the final construct.

5.2.2. Production of pcDNA3-HA-NLRP7 and pcDNA3-FLAG-NLRP7 Constructs

The FLAG and HA-tagged NLRP7 constructs were generated by modifying the pcDNA3-MYC-NLRP7 construct. MYC- tag was removed by digestion with restriction enzymes Xba I and Nde I. The desired 8000 bp vector backbone containing NLRP7 was isolated from the agarose gel and ligated to FLAG and HA tags that were removed from empty FLAG and pcDNA3-HA vectors by Xba I and Nde I digestion. Analytical restriction digestion confirmed the successful cloning of the FLAG and HA-tagged versions of NLRP7. Constructs were sequenced to confirm corrections of sequences (Figure 5.5).

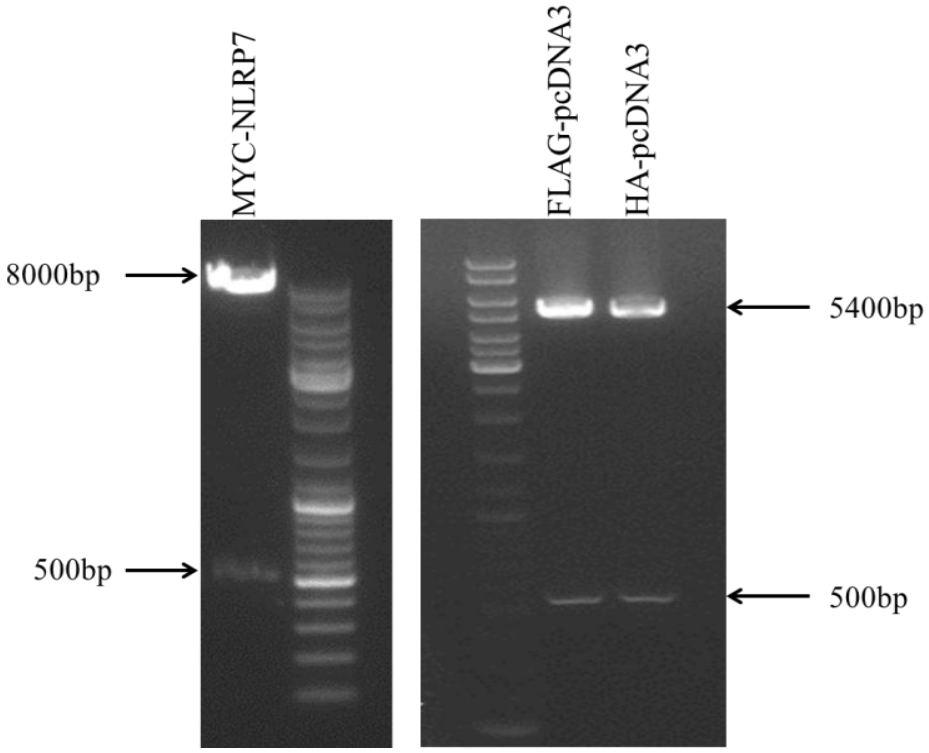

Figure 5.5. Cloning of NLRP7 into pcDNA3-FLAG and pcDNA3-HA from pcDNA3-MYC.

5.2.3. Production of pEGFP-C3-NLRP7 Expression Construct

The EGFP-NLRP7 fusion construct was generated to assess the localization of NLRP7 using fluorescent microscope. For this purpose, the NLRP7 fragment was obtained from the Tag-RFP-T-NLRP7 plasmid (made by A. Sahillioglu) by digestion with Not I, followed by partial digestion with Sac I (Figure 5.6a). pEGFP-C3-ASC plasmid was digested with Sac I and Not I to remove ASC and replace it with NLRP7 (Figure 5.6b) and ligated to NLRP7. Two positive colonies (2 and 3) were selected according to their EcoR I analytical digestion banding pattern (Figure 5.6c) and sequenced to confirm the final construct.

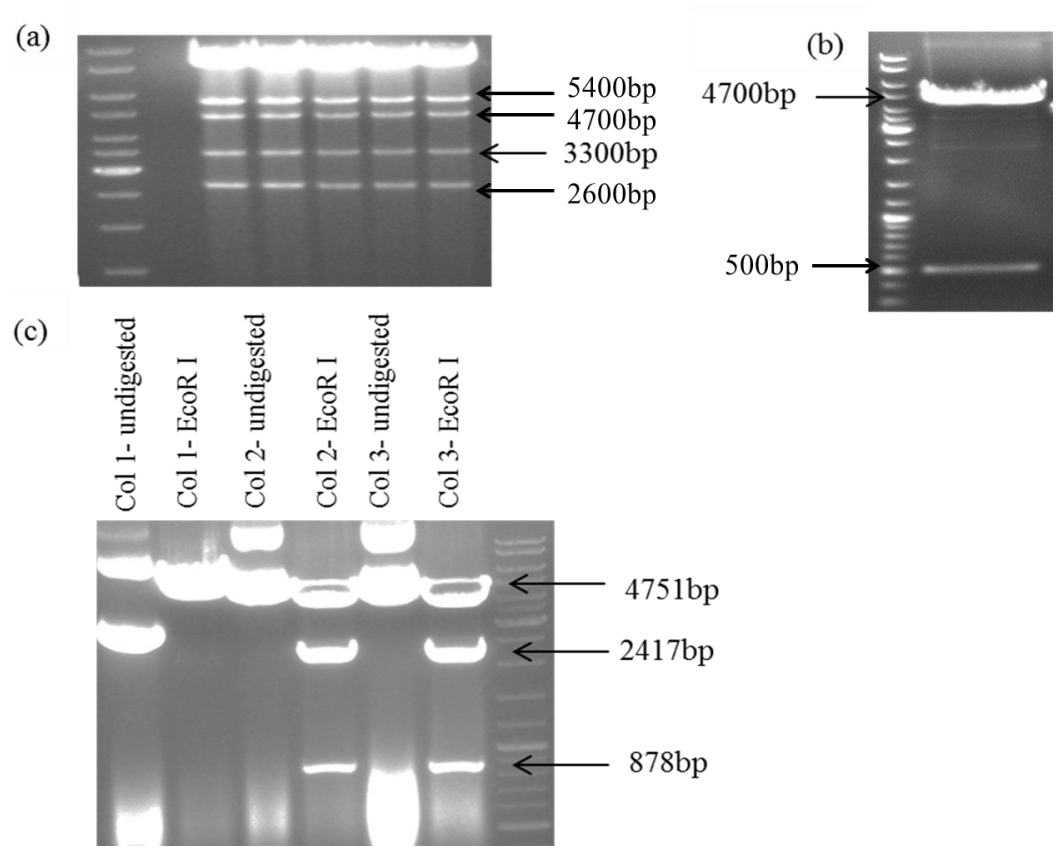

Figure 5.6. Cloning of NLRP7 into pEGFP-C3 vector. (a) Isolated band after Tag-RFP-T NLRP7 digestion (b) Isolated band after pEGFP-C3-ASC digestion (c) Analytic digestion of pEGFP-C3-NLRP7 (d) Map of the final construct.

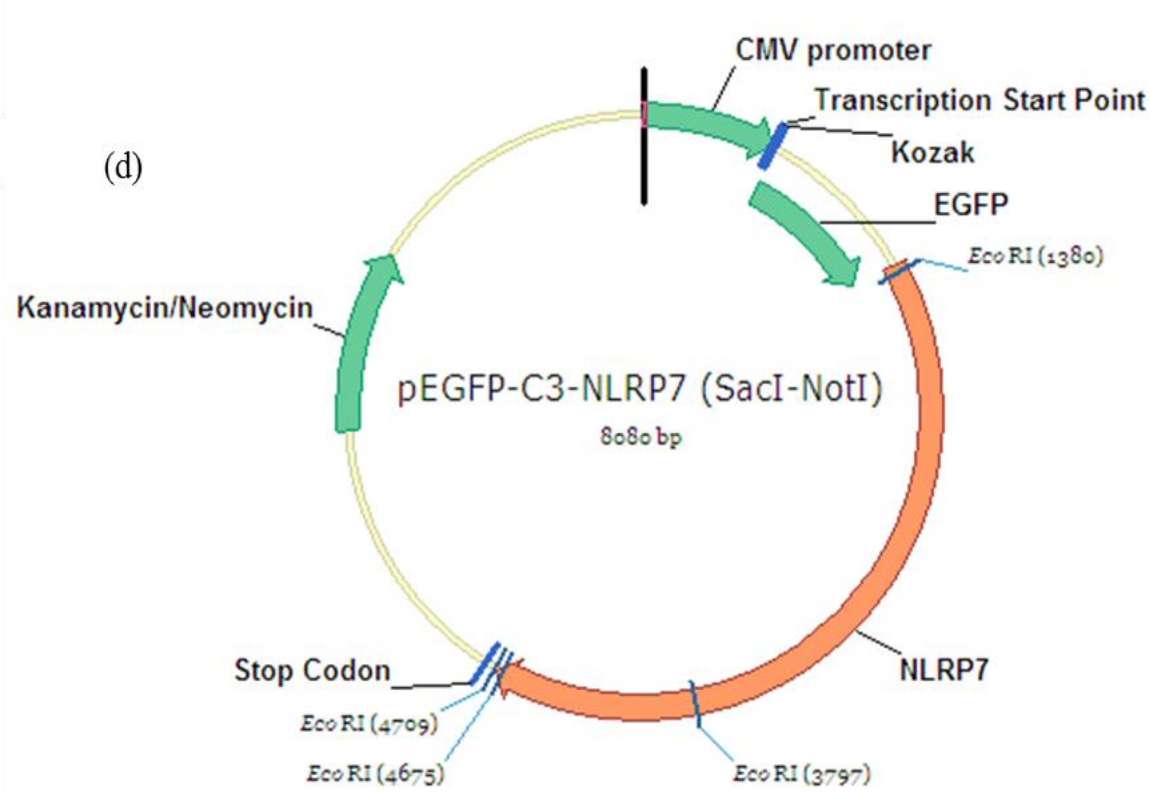

Figure 5.6. Cloning of NLRP7 into pEGFP-C3 vector. (a) Isolated band after Tag-RFP-T NLRP7 digestion (b) Isolated band after pEGFP-C3-ASC digestion (c) Analytic digestion of pEGFP-C3-NLRP7 (d) Map of the final construct (cont.).

5.2.4. Production of pLenti-Ef1a-RFP-NLRP7 Construct

This lentiviral RFP-NLRP7 fusion construct was generated to produce RFP-NLRP7 expressing stable cell lines. The Tag-RFP-T-NLRP7 (generated by A. Sahillioglu) vector was digested with Nhe I and Not I in order to take out RFP-fused NLRP7 (Figure 5.7a). At the same time pLenti-EF-1a plasmid was digested with Nhe I and partially with Not I and ligated to N-terminally-RFP fused NLRP7. Analytic digestion with EcoR I (Figure 5.7b) showed the presence of two positive colonies. Both were sent to sequencing to confirm correctness of the construct (Figure 5.7c).

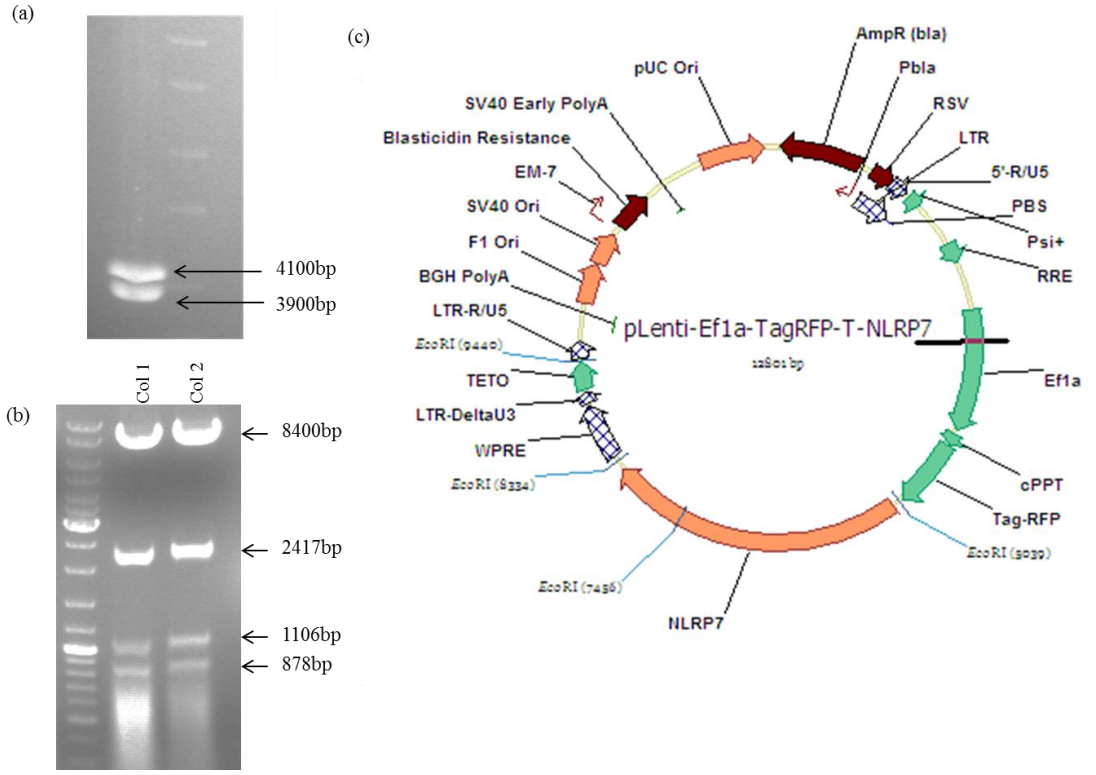

Figure 5.7. Cloning of RFP-NLRP7 fusion protein into pLenti-EF1a vector. a) 4100bp band isolated after Tag-RFP-T NLRP7 plasmid digestion b) Analytic digestion of pLenti-EF1a-TagRFP-T-NLRP7 plasmid c) Map of the final construct.

5.2.5. Production of pLenti-Ef1a-EGFP-NLRP7 Construct

This lentiviral EGFP-NLRP7 fusion construct was generated to produce EGFP-NLRP7 expressing stable cell lines. The pEGFP-C3-NLRP7 vector was digested with Nhe I and Not I in order to take out EGFP-fused NLRP7 (Figure 5.8a) and ligated to pLenti-EF-1a plasmid. Analytic digestion with EcoR I (Figure 5.8b) revealed two positive colonies that were selected for further analysis by sequencing. Sequences were confirmed to finalize the construct (Figure 5.8c).

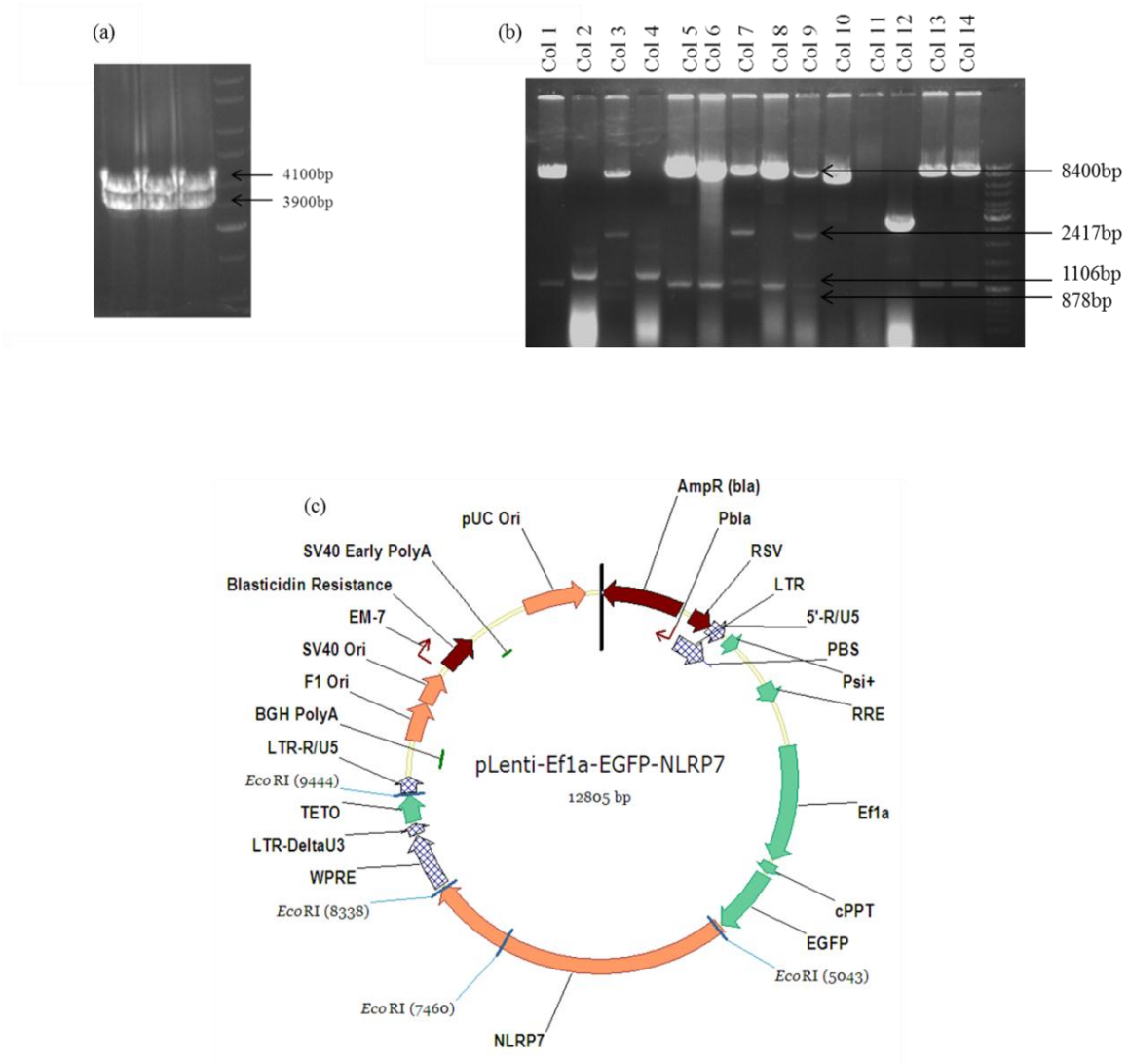

Figure 5.8. Cloning of EGFP-NLRP7 fusion protein into pLenti-EF1a vector. a) 4100bp band isolated after pEGFP-C3- NLRP7 plasmid digestion b) Analytic digestion of pLenti-EF1a-EGFP-NLRP7 plasmid c) Map of the final construct.

5.3. Confirmation of Tagged NLRP7 Protein Expression in HEK293FT Cell Line

The HEK293FT is a widely used and invaluable cell line for expressing proteins in cell culture. HEK293FT cells were transfected with various amounts of each of MYC-, FLAG- or pcDNA3-HA-NLRP7 using pEGFP-C3 as a transfection control in 6-well plates via calcium phosphate transfection method. As the transfection efficiency was above 80% on the next day (Figure 5.9a), the cells were harvested and samples were run on SDS-PAGE for Western Blotting (Figure 5.9b). Then immunoblotting was performed by using tag-specific antibodies, ie. anti-MYC, anti-FLAG and anti-HA and also anti-actin primary antibodies and HRP linked-anti-rabbit secondary antibody. It is clear that all three differently tagged versions of NLRP7 are expressed at the expected 120kDa size.

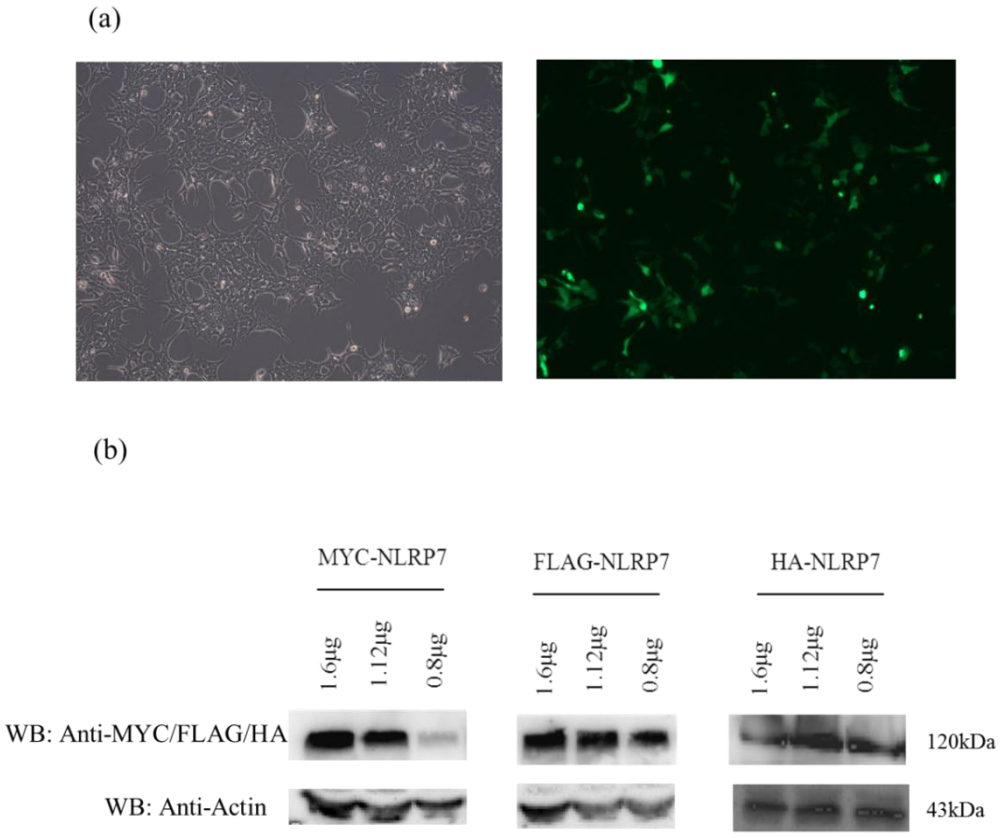

Figure 5.9. Expression of pcDNA3 clones (a) Representative figure for transfection efficiency MYC-NLRP7 co-transfected with EGFP-C3 (b) Blot of tagged-NLRP7 overexpression in HEK293FT cells. All tagged versions are expressed.

5.4. Cellular Localization of NLRP7

The cellular localization of a protein also reflects its function. Since there is very little knowledge about NLRP7 and its functions, we aimed to clarify its cellular localization. For this purpose, the EGFP-NLRP7 fusion construct was co-transfected with various constructs encoding markers for subcellular structures including ECFP-Rab5, ECFP-Rab9, ECFP-Rab11 and dsRED mitochondrial marker separately into HEK293FT cells via calcium phosphate transfection. Following transfection the cells were fixed and visualized with the confocal microscope. For calculation of percent co- localizations only cells that seem to be alive were counted using pictures taken from different areas of the same sample.

Many of the known NLR family members are also cytosolic proteins with the exception of nuclear CIITA and mitochondrial NLRX1. In order to clarify whether NLRP7 could also get localized in these compartments, the subcellular localization experiments were carried out. As expected, EGFP-NLRP7 was found to be widely spread in the cytoplasm. On the other hand endosomes and mitochondria showed stainings concentrated at certain points. DAPI was used for nuclear staining.

Rab 5, an early endosome marker, was found to co-localize with NLRP7 in almost 5% of the cells (Figure 5.10).

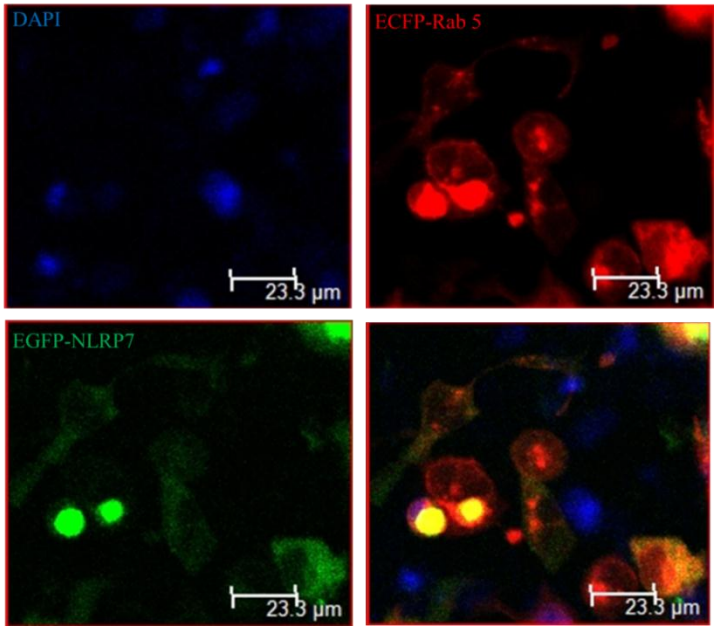

Figure 5.10. Co-localization of NLRP7 with early endosomal marker Rab 5.

NLRP7 co-localized with late endosome marker Rab9 in less than 5% of the cells (Figure 5.11).

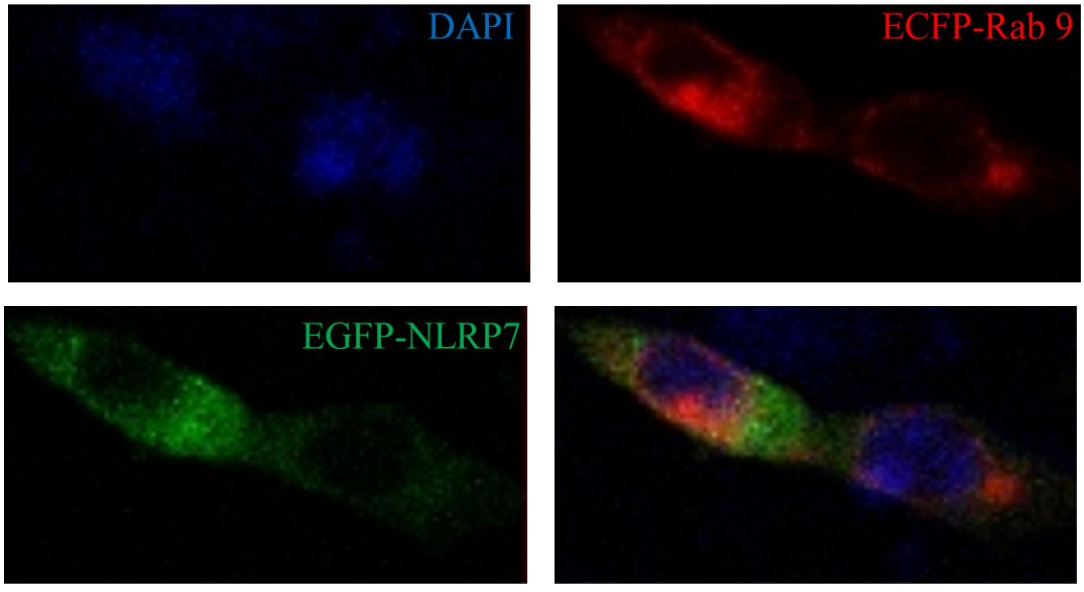

Figure 5.11. Colocalization of NLRP7 with late endosomal marker Rab 9.

NLRP7 co-localized with recycling endosome marker Rab11 in less than 5% of the cells (Figure 5.12).

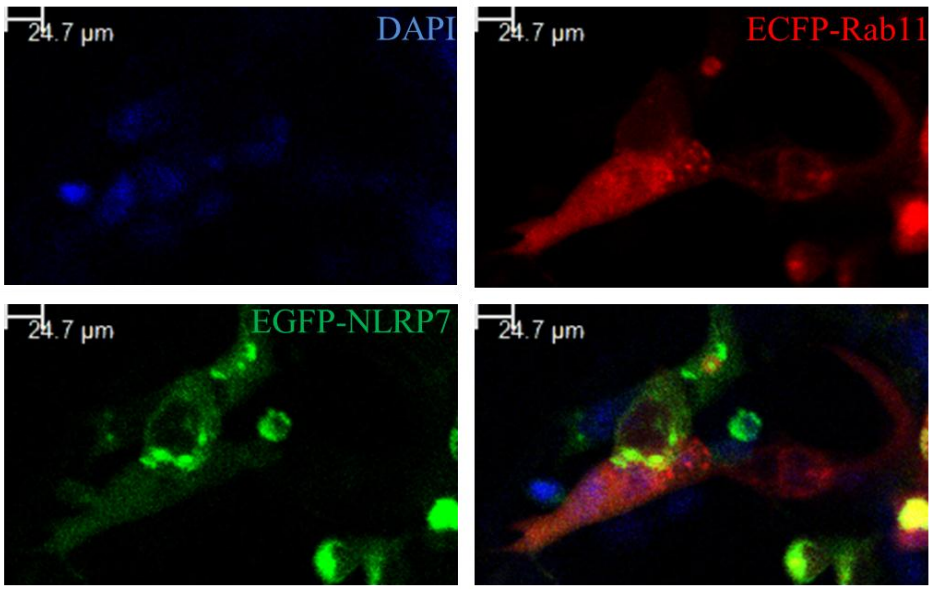

Figure 5.12. Co-localization of NLRP7 with the recycling endosome marker Rab 11.

On the other hand, NLRP7 was found to co-localize with mitochondrial marker in 25% of the cells (Figure 5.13).

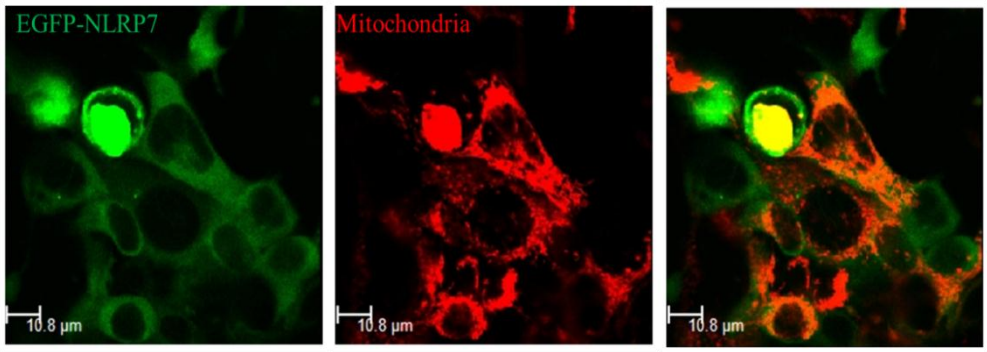

Figure 5.13. Co-localization of EGFP-NLRP7 with dsRED mitochondrial marker.

As a result we conclude that NLRP7 is a predominantly cytosolic protein with minor localization with mitochondria.

5.5. Co-localization of NLRP7 with Inflammasome Components

NLR proteins may exert their function by forming inflammasomes, thus, co-localization of NLRP7 with building blocks of the inflammasome complex was examined. For this purpose EGFP-NLRP7 was co-transfected with ECFP-Caspase-1 and/or RFP-ASC separately and in combination (Figure 5.14). Caspase-1 was found to be dispersed through the cytoplasm as much as NLRP7 upon overexpression in HEK293FT cells. However, upon co-transfection with ASC, NLRP7 perfectly co-localizes with ASC in ASC-formed-specks where NLRP7 also spread in the cytoplasm. Most importantly when ASC, Caspase-1 and NLRP7 co-transfeceted, they co-localize in the cytoplasm, forming inflammasome-like structures.

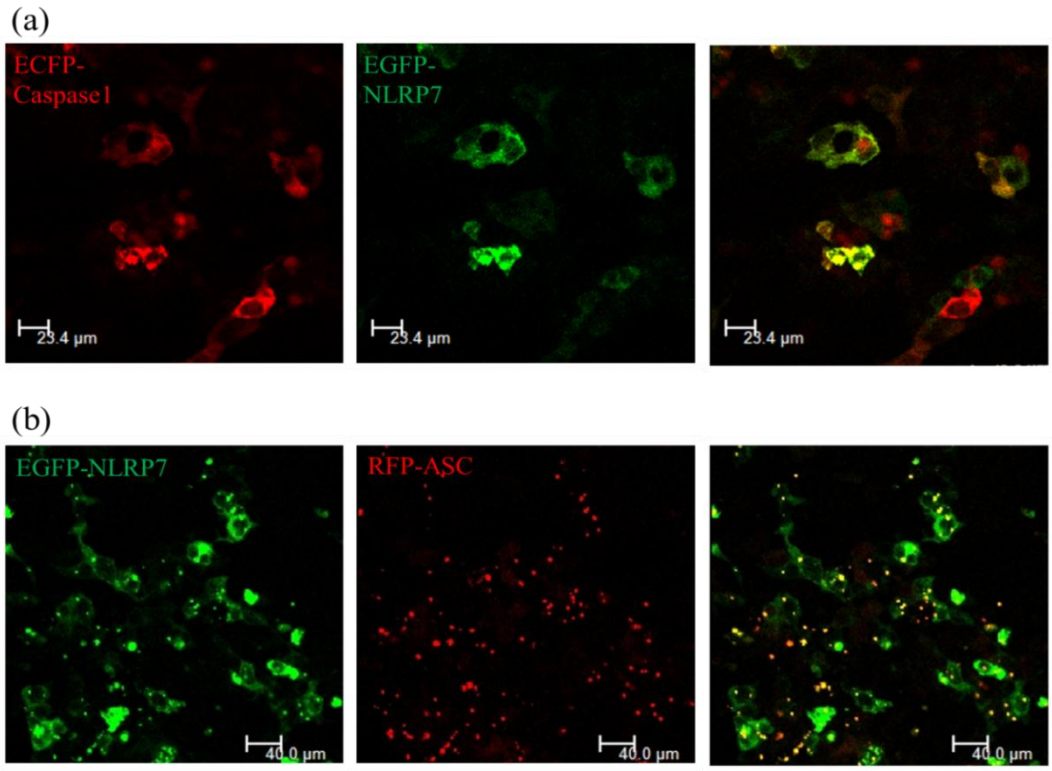

Figure 5.14. NLRP7 co-localizes with Caspase-1 and ASC in speck structures. (a) Caspase-1 and NLRP7 co-localization (b) ASC and NLRP7 co-localization (c) Caspase-1, ASC and NLRP7 co-localization.

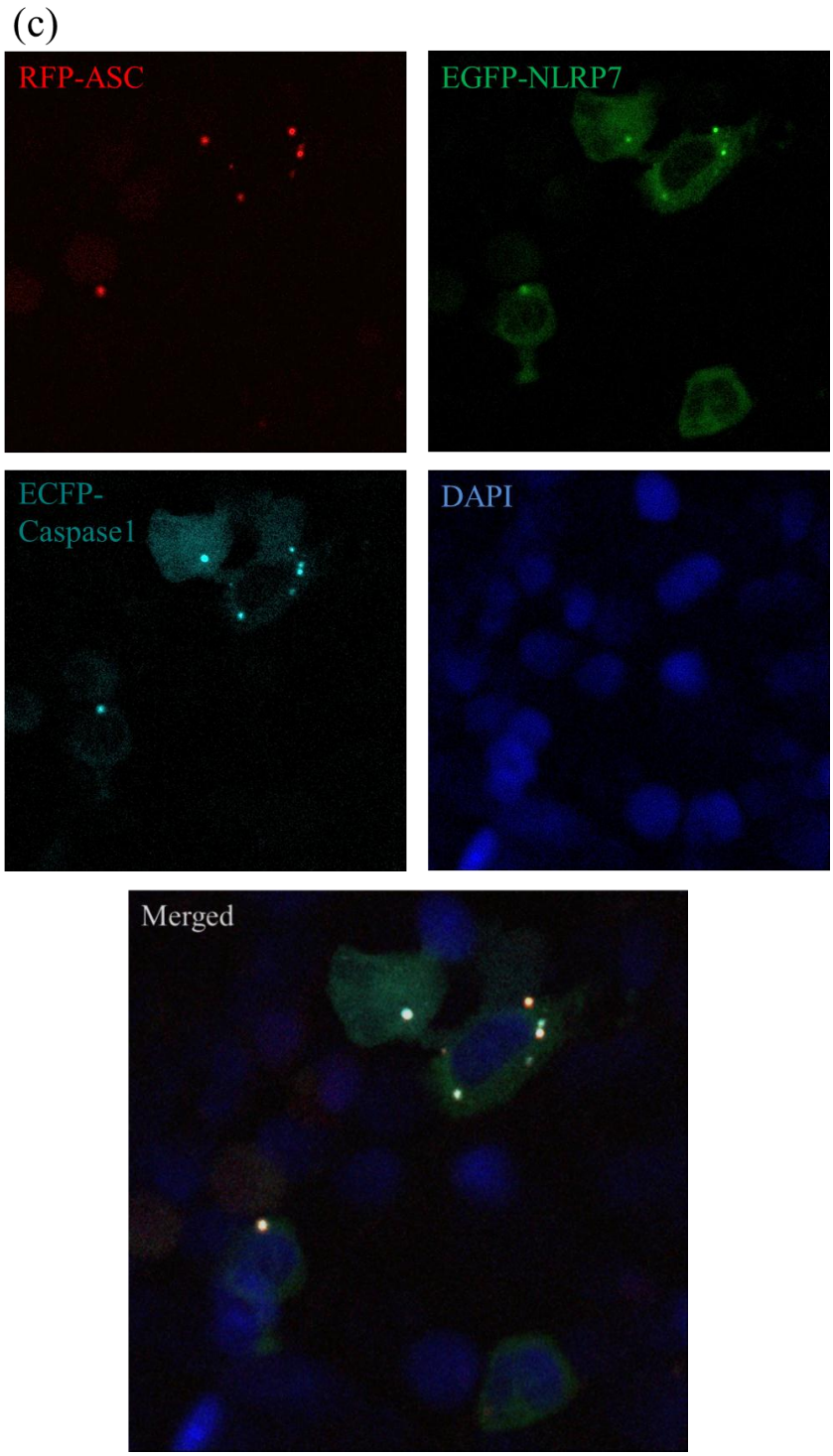

Figure 5.14. NLRP7 co-localizes with Caspase-1 and ASC in speck structures. (a) Caspase-1 and NLRP7 co-localization (b) ASC and NLRP7 co-localization (c) Caspase-1, ASC and NLRP7 co-localization (cont.).

5.6. Interaction of NLRP7 with Caspase-1, Caspase-5, ASC

5.6.1. NLRP7 Interacts with Caspase-1

NLRs may form inflammasomes for activating Caspase-1 and Caspase-5, for which NLRs may or may not need the adaptor ASC protein. To test whether NLRP7 can directly bind to Caspase-1 co-immunoprecipitation was performed in HEK293FT cells after transfection with NLRP7 and Caspase-1. 48h after transfection the cells were harvested and Co-IP was carried out using anti-FLAG antibody to precipitate FLAG-Caspase-1 followed by Western blotting using anti-MYC antibody in order to detect FLAG-Caspase-1 bound MYC-NLRP7 (Figure 5.15) and from these experiments it became clear that NLRP7 can interact with caspase-1 but this interaction appears quite weak.

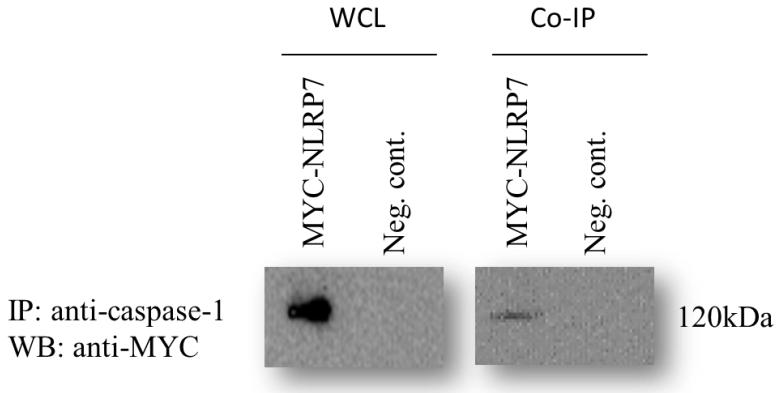

Figure 5.15. Interaction of NLRP7 with Caspase-1. WCL: Whole Cell Lysate, Co-IP: Co-Immunoprecipitation. (Figure represents three independent experiments)

5.6.2. NLRP7 Interacts with Caspase-5

In order to test whether NLRP7 has the potential to interact with caspase-5, both proteins were overexpressed in HEK293FT cells in their tagged forms, namely MYC-NLRP7 and FLAG-caspase-5. Cell lysates were immunoprecipitated using anti-FLAG antibody, followed by Western blotting with anti-MYC antibody (Figure 5.16). Clearly, NLRP7 found to interact with caspase-1 and caspase-5 in the absence of ASC.

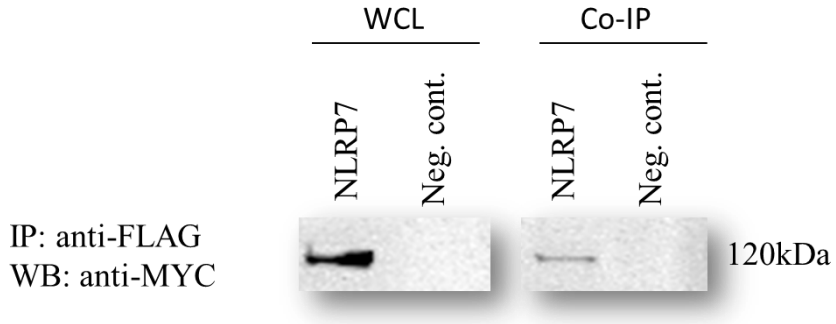

Figure 5.16. Interaction of NLRP7 with caspase-5. WCL: Whole Cell Lysate, Co-IP: Co-Immunoprecipitation. (Figure represents three independent experiments)

5.6.3. NLRP7 Interacts with ASC

In order to test whether NLRP7 has the potential to interact with ASC, both proteins were overexpressed in HEK293FT cells in their tagged forms, namely MYC-NLRP7 and FLAG-ASC. For this purpose the cell lysates were immunoprecipitated using anti-FLAG antibody, followed by Western blotting (Figure 5.17) and interestingly, NLRP7 has the capacity to interact with ASC under overexpression conditions that were used.

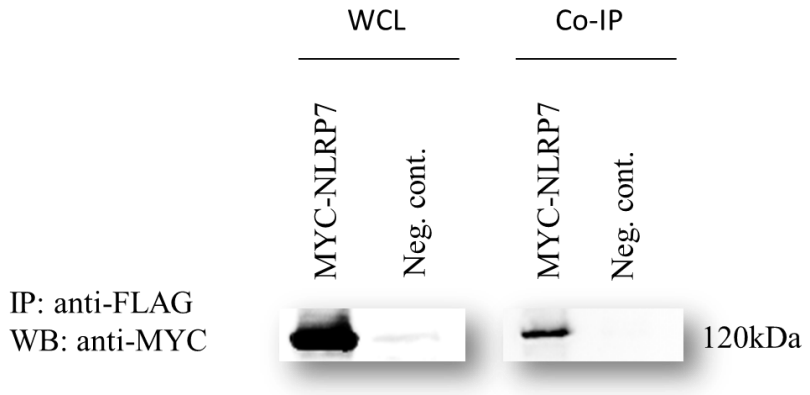

Figure 5.17. Interaction of NLRP7 with ASC. WCL: Whole Cell Lysate, Co-IP: Co-Immunoprecipitation. (Figure represents three independent experiments)

5.7. Inflammasome Activation

The observed interaction of NLRP7 and caspase-1 and ASC and its co-localization with ASC and caspase-1 suggested that NLRP7 may form an inflammasome. To test this hypothesis 1 µg of each of the inflammasome components, including ASC, caspase-1 and IL-1β were co-transfected into HEK293FT cells in addition to 1 µg NLRP7 and IL-1β processing by caspase-1 inside the cell was measured via Western Blotting and the bands were quantified using Image J software (Figure 5.18). The positive control of this experiment was NLRP3 and as expected IL-1β maturation was quite pronounced (lane 1) compared to negative control (lane 6). When NLRP7 was added instead of NLRP3, it was observed that IL-1β maturation was almost as high as the positive control (lane 3). Although in the absence of ASC, mature IL-1β levels decreased (lane 4), it was higher than the sample with NLRP3 (lane 2). Overall these data suggested that NLRP7 forms an IL-1β maturating inflammasome which is not dependent on ASC, although IL-1β maturation increases in the presence of ASC.

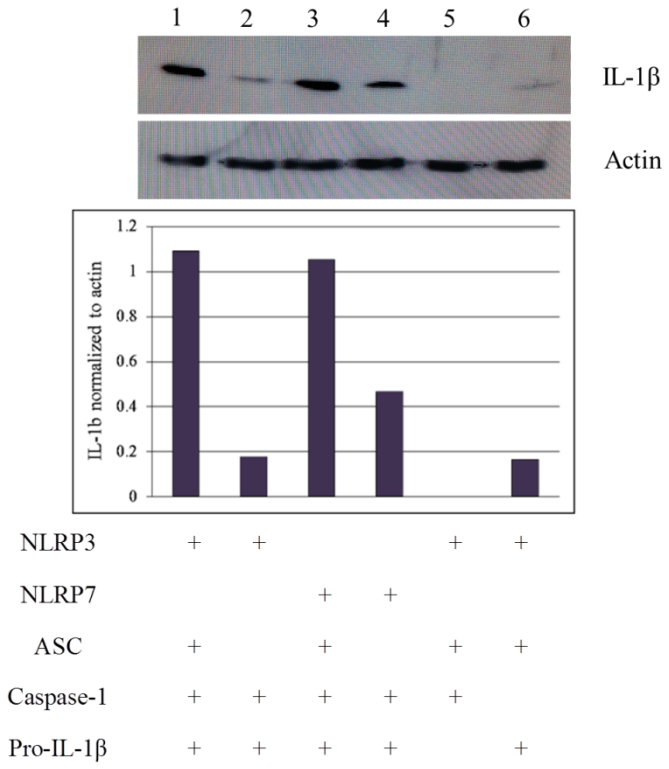

Figure 5.18. NLRP7 overexpression leads to pro-IL-1β processing.

5.8. Generation of Stable NLRP7-Knock-down HEC-1-A Cell Line

In order to detect the possible roles of NLRP7 in various pathways, NLRP7 levels were stably knocked down in an endogenously NLRP7 expressing cell line- HEC-1-A using lentiviruses. The viruses were produced in HEK293FT cells via calcium phosphate transfection using commercially available four shRNA and one scrambled lentiviral plasmids and related packaging vectors (Figure 5.19). The viruses were used to infect HEC-1-A cells selected for puromycin resistant stably shRNA expressing cells (Figure 5.20). Four shRNA plasmids were used to stably transduce the HEC-1-A cells whereas scrambled RNA plasmid transduction was used as a control.

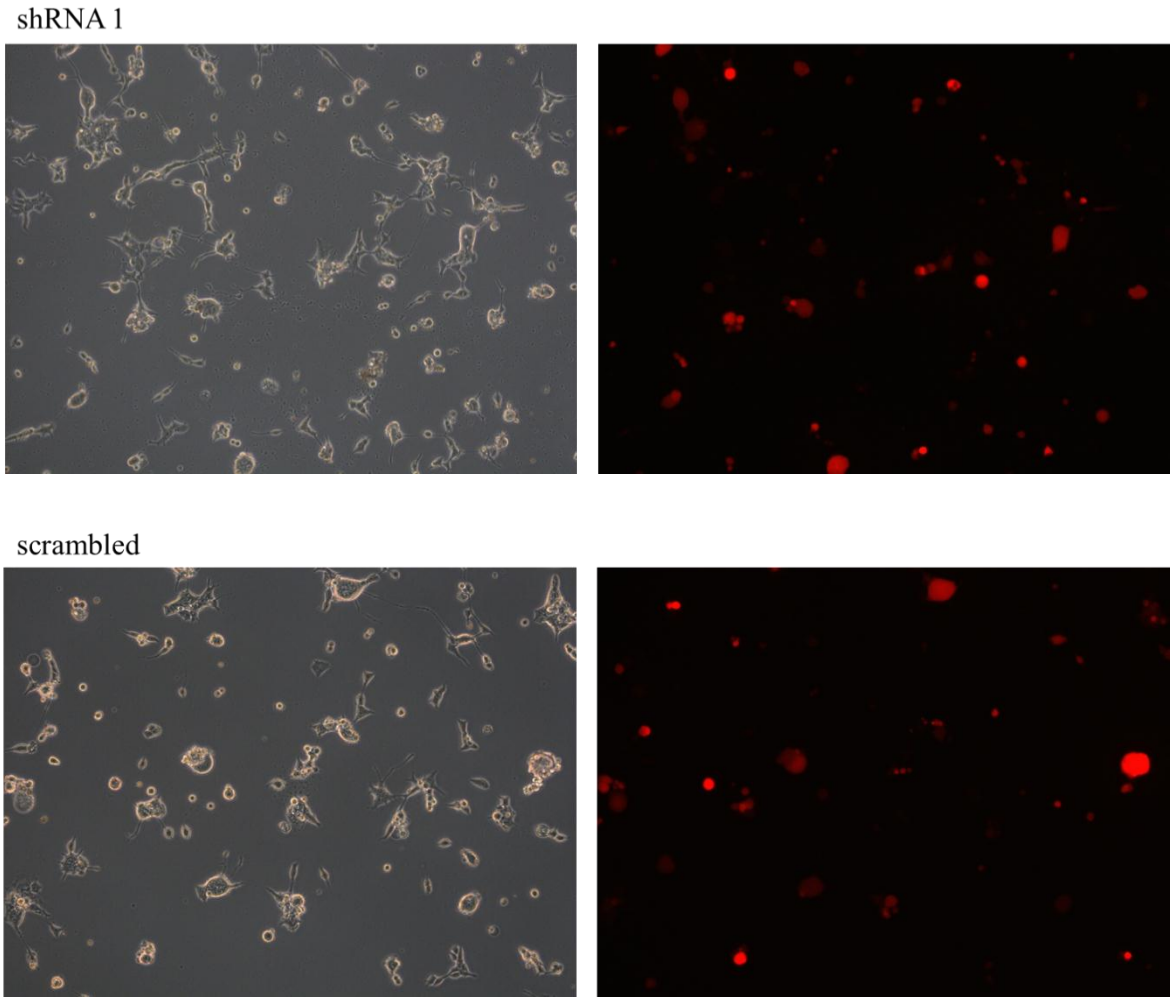

Figure 5.19. Lentivirus production in HEK293FT cells.

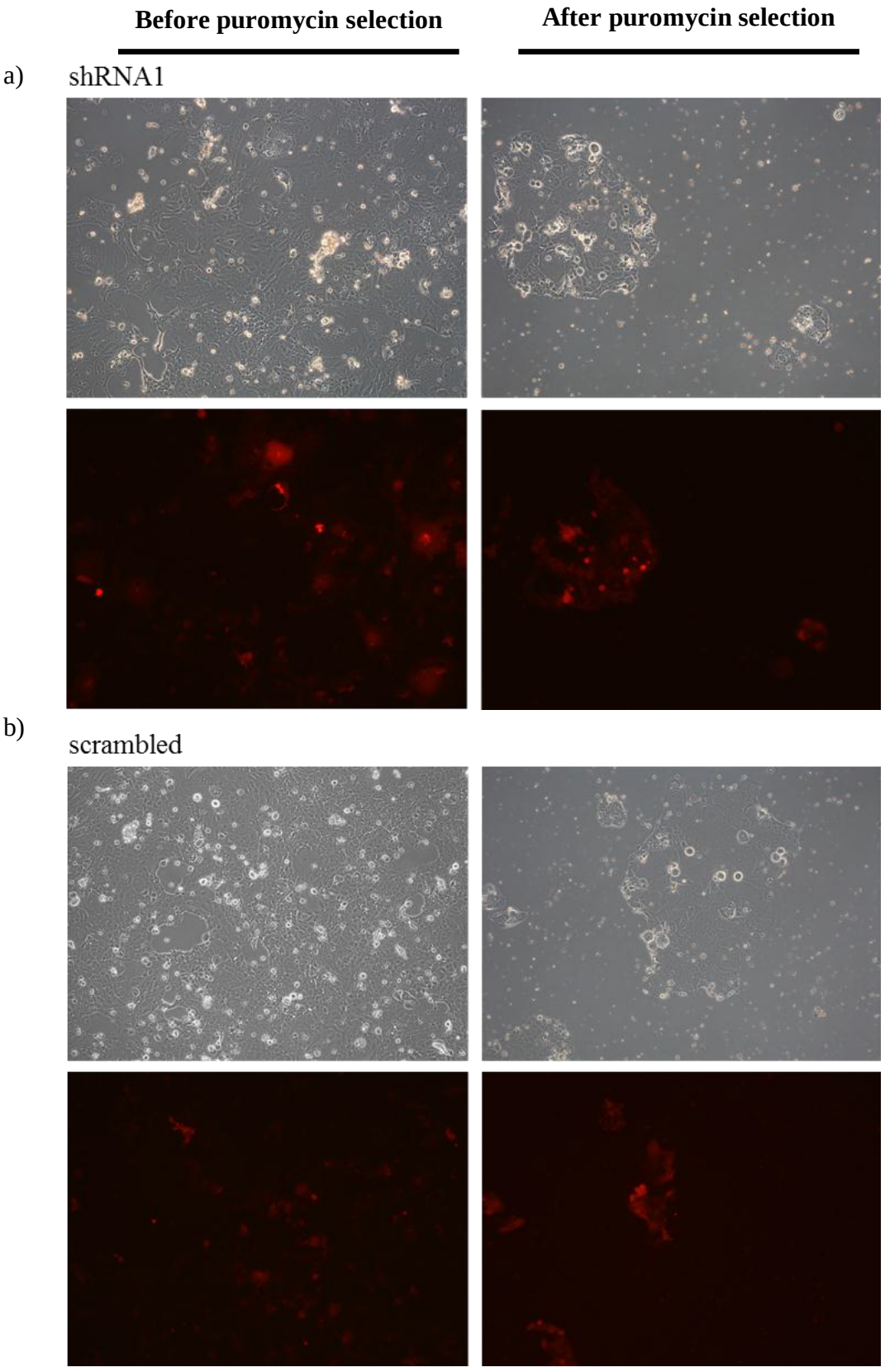

Figure 5.20. Generation of stable NLRP7 shRNA expressing HEC-1-A lines.

5.9. Stable NLRP7 Knock-Down in HEC-1-A Cells Leads to a Reduction in TNF-R2, TWEAK, TRAIL-R3, p53 and IL-1β and Upregulation in Fas Transcript Levels

In order to detect the role of NLRP7 in immune privilege, the effect of four different shRNA constructs were tested (Figure 5.21) and sh1 was selected for the most prominent reduction in NLRP7 RNA levels (75%). The effects of NLRP7 knock-down in HEC-1-A cell line on death receptors were determined at the messenger RNA level. For this purpose, following isolation of total RNA, cDNA was produced with RT-PCR followed by Q-PCR using gene specific primers in triplicates (Figure 5.22). EF-1α was used as an internal control to the real-time PCR reactions and each sample was normalized to EF-1α. Each reaction was performed separately in scrambled and shRNA expressing HEC-1-A cell lines and taking scrambled samples as one, all the knock down samples were shown in folds. Eventually, making sure that negative control reaction with ddH_2O had a cycle number larger than or equal to 35 ($n \geq 35$), in response to 90% down-regulation of NLRP7, TNF-R2 showed 40%, TWEAK showed 30%, TRAIL-R3 showed 50%, p53 showed 40% and IL-1β showed 80% decrease whereas Fas showed 10% increase in transcript levels in comparison to scrambled controls with the same primers.

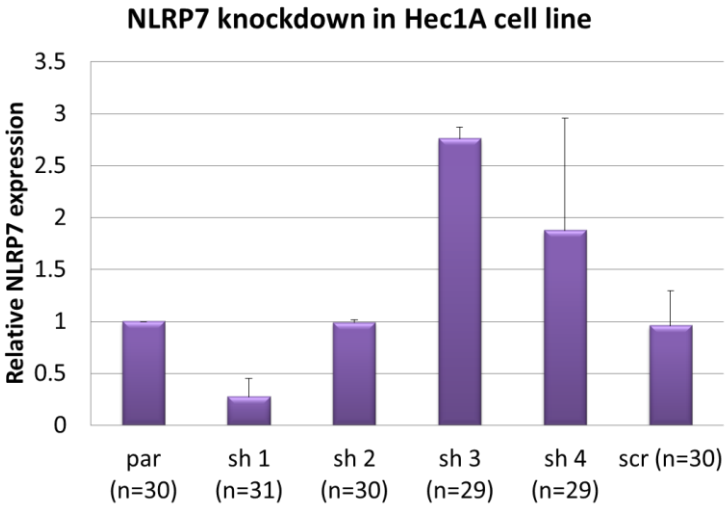

Figure 5.21. Knock-down of NLRP7 transcript via shRNA in HEC-1-A cells. n: cycle number

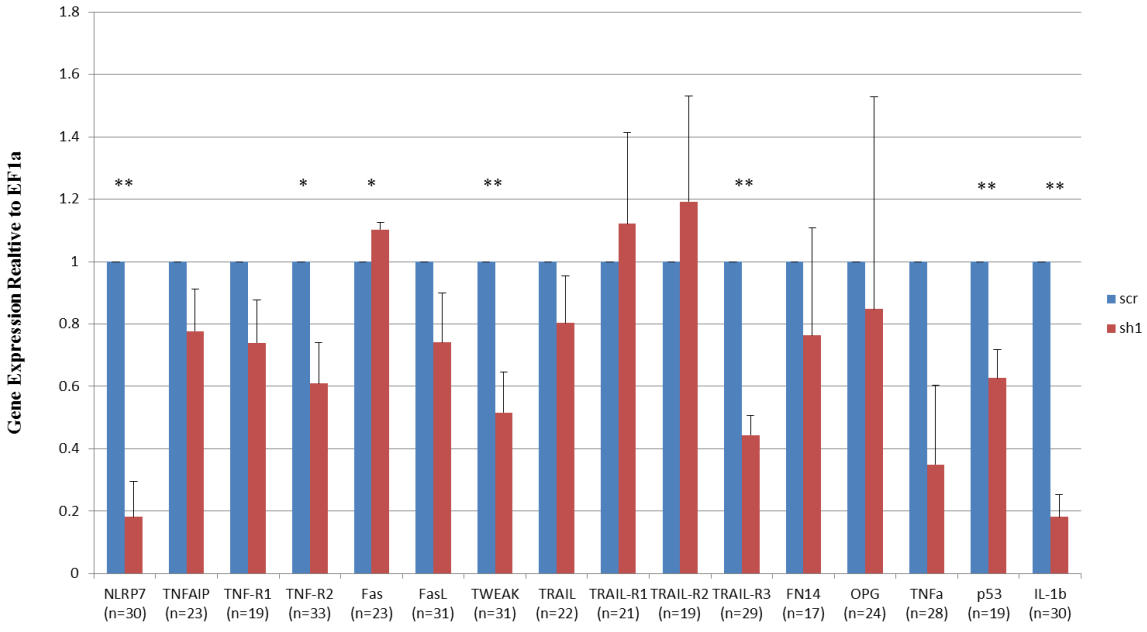

Figure 5.22. NLRP7 knock-down causes a shift in the expression of certain genes. Each average Ct value of one triplicate then normalized with corresponding EF1a Ct value. n: cycle number of scrambled, *: $p<0.05$ **: $p<0.01$

5.10. Study of Death Receptors or Surface HLA Profile Change in NLRP7 Knock-Down HEC-1-A Cell Line by FACS

5.10.1. Flow Cytometric Analysis of Death Receptors and Ligands

In order to see whether the gene expression changes detected by Q-RT-PCR result in changes of protein levels on the cell surface, death receptors and ligands, that were found to be changed upon NLRP7 knock-down, were measured using flow cytometry as well after surface staining using fluorochrome labeled antibodies. According to that, Fas receptor levels were also upregulated at the protein level whereas TNF-R2, TWEAK, TRAIL-R3 and also FasL and TRAIL did not vary in comparison to real time data (Figure 5.23). In fact the only consistent finding was related with Fas expression levels, which were found to be upregulated once NLRP7 was knocked down.

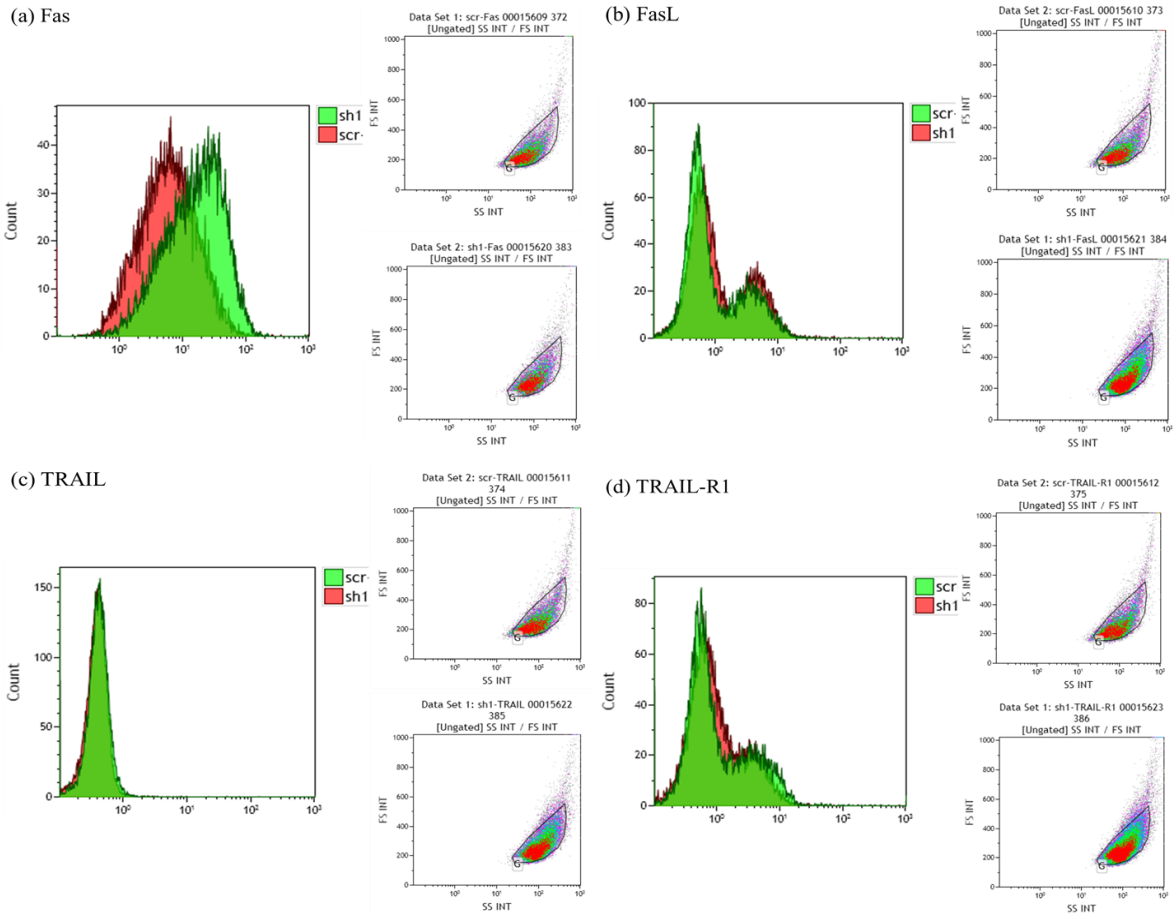

Figure 5.23. Effect of NLRP7 knock-down on death ligand and death receptor expression. (a) Fas (b) FasL (c) TRAIL (d) TRAIL-R1 (e) TRAIL-R3 (f) TNF-R2 (g) TWEAK.

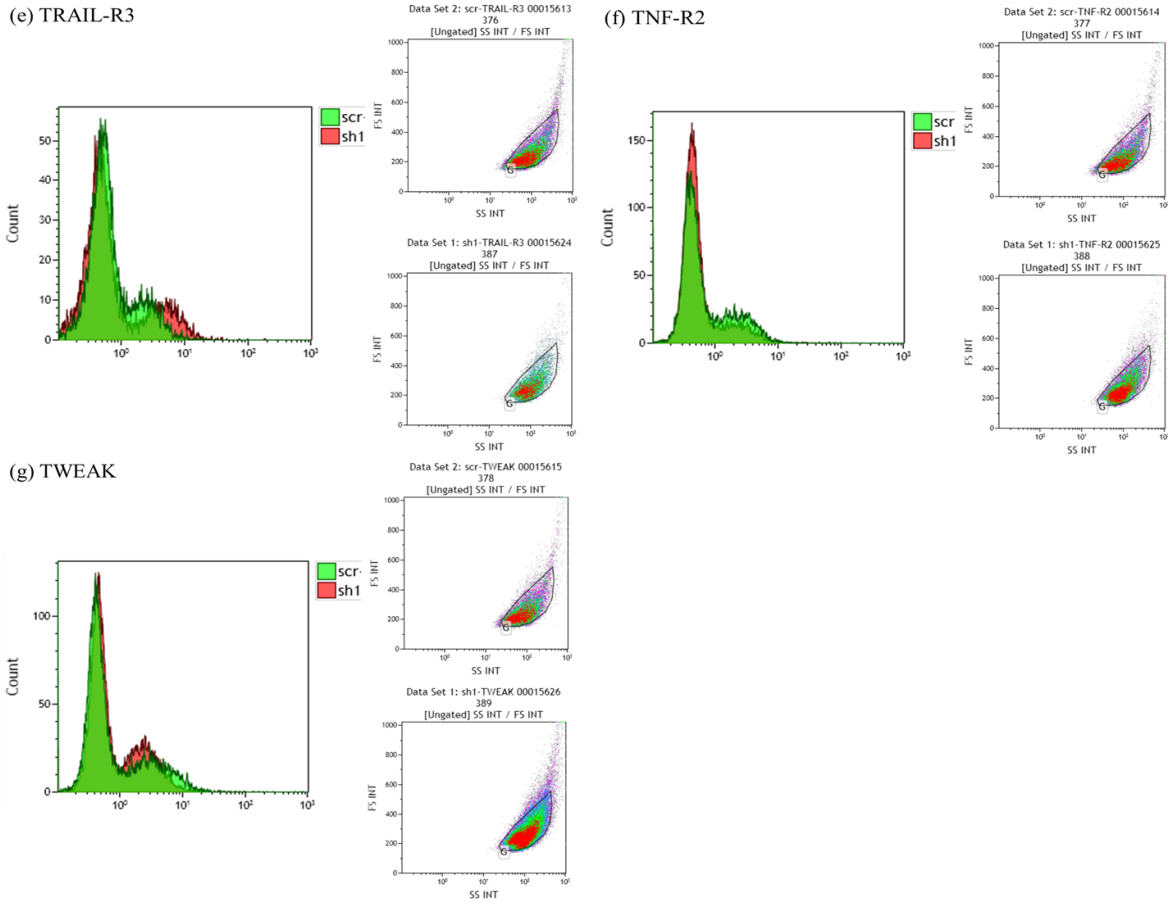

Figure 5.23. Effect of NLRP7 knock-down on death ligand and death receptor expression. (a) Fas (b) FasL (c) TRAIL (d) TRAIL-R1 (e) TRAIL-R3 (f) TNF-R2 (g) TWEAK (cont.).

5.10.2. Flow Cytometric Analysis of HLA Proteins

One of the main characteristics of immune privileged sites is the shift of HLA molecules from HLA A, B, C type to HLA E and G type. Thus, the protein levels of HLA molecules were measured and compared using flow cytometry (Figure 5.24) after surface staining using fluorochrome labeled antibodies in parental and stable NLRP7 knock-down HEC-1-A cells. It was found that HLA A, B, C levels decrease in stably NLRP7 specific shRNA expressing HEC-1-A cells when compared to scrambled RNA expressing HEC-1-A cells whereas HLA E and HLA G do not change.

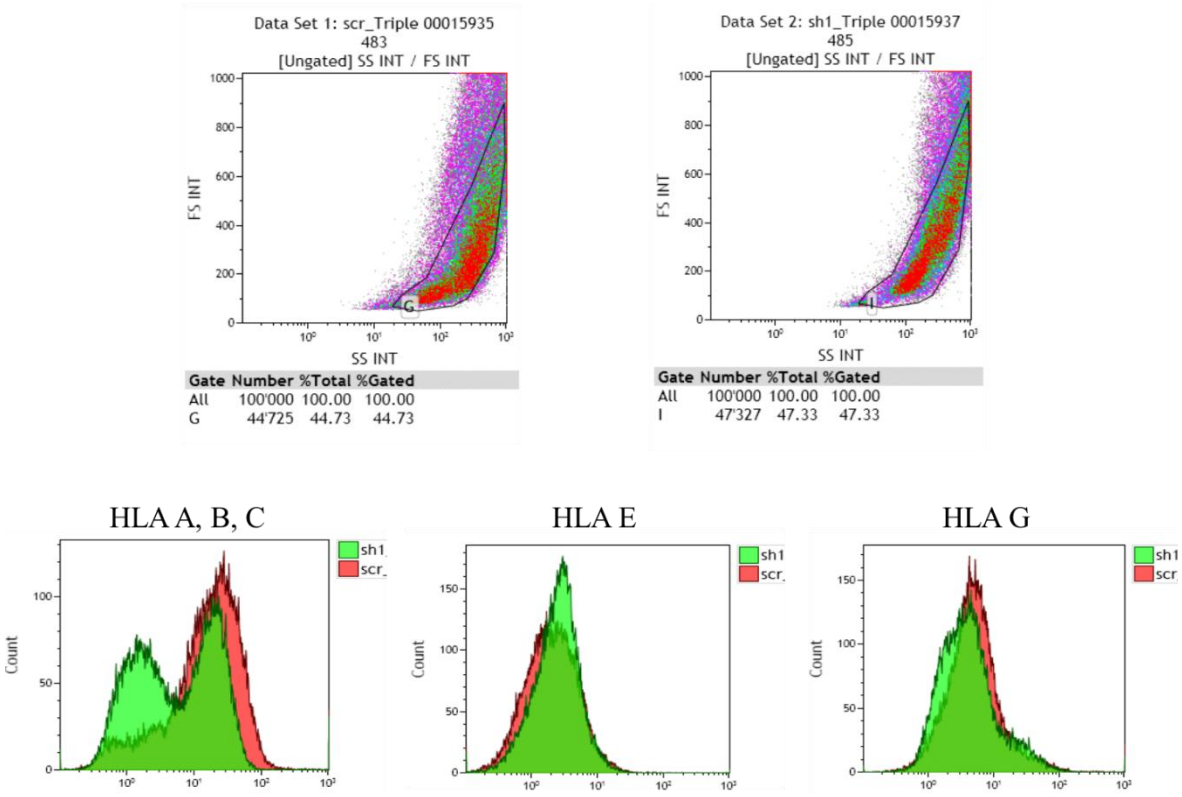

Figure 5.24. HLA A, B, C expression decrease but HLA E and G expression do not change on the surface of HEC-1-A cells upon NLRP7 knock-down. The figure is the representative of three independent experiments

5.11. NLRP7 has no Effect on NF-κB Driven Transcription

In addition to the possible roles stated above, NLRs are also known to act on the NF-κB signaling pathway. Therefore, utilizing the luciferase assay, the influence of NLRP7 on NF-κB activation was determined. Varying amounts of NLRP7 plasmid was co-transfected with constant amount of NOD1, which is known to activate NF-κB signaling, together with firefly luciferase and renilla plasmids. After that, first firefly luciferase then renilla substrates were added and each firefly luciferase measurement was normalized with renilla measurement. Experiments were performed in triplicates and each measurement was calculated by taking average of five readings. Increasing concentrations of NLRP7 showed no effect on NOD1 induced NF-κB activation (Figure 5.25) although positive control NOD 1 increased renilla normalized NF-κB activity 150 fold, taking negative control with neither NLRP7 nor NOD1 as one fold. On the other hand NLRP7 alone did not cause any NF-κB activation (0.8 fold) and increasing amounts of NLRP7 had no significant effect on NF-κB inhibition.

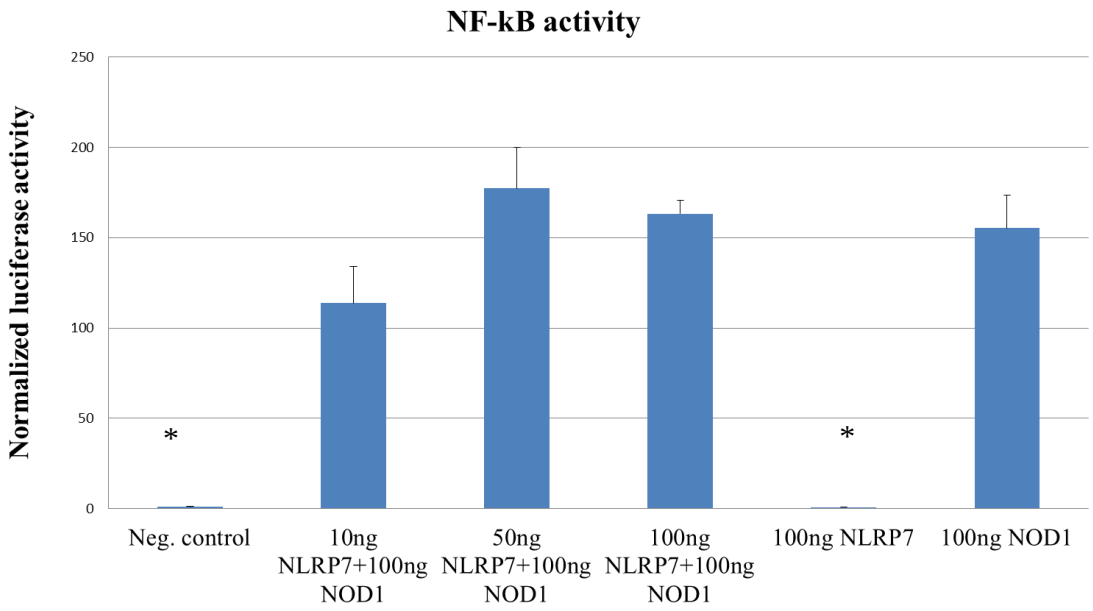

Figure 5.25. Effect of NLRP7 on NF-κB activation. Representative figure of three independent repeats.

6. DISCUSSION

NLRP7 is a novel protein which deserves further study. NLRP7 has an N-terminal PYRIN domain, a central NACHT domain and a C-terminal LRR domain (Figure 5.1). It is expressed only in primates, among which it is extremely conserved (Figure 5.2).

NLR family members have functions in inflammatory and apoptotic pathways. They may fulfill their function either alone, like NOD1 and NOD2 or by forming multi-protein structures that activate Caspase-1 called inflammasomes like NLRP1, NLRP3 and NLRC4. Upon ligand binding NOD1 and NOD2 acquire structural changes causing recruitment of the serine-threonine kinase RICK followed by TAK1 kinase that is required for MAPK and IKK activation and eventually MAPK and NF-κB pathway activations, respectively (Shaw *et al.*, 2008). In order to understand whether NLRP7 has any effect on NF-κB activation, luciferase assays were performed using NOD1 as a signal activator (Figure 5.25). Our results show that NLRP7 does not alter NOD1 induced NF-κB activity.

Another possibility for NLR function could be the formation of scaffolds for Caspase-1 and sometimes for Caspase-5 activation, namely inflammasomes. This structure is thought to be synonymous to the apoptosome structure that is important for the activation of caspase-9 during apoptosis. In the apoptosome APAF1 molecules form a scaffold upon cytochrome C binding, which is followed by pro-caspase-9 recruitment and activation. In the case of inflammasomes, however an NLR protein takes the place of APAF1. This NLR may need the adaptor protein ASC for homophylic binding to Caspase-1 or may not (as in the case of CARD containing NLRC 4). Out of the three NLR proteins thus far confirmed to form inflammasomes, the NLRP3 inflammasome is the best characterized one and it is known to require ASC to bind and form the molecular port for Caspase-1 binding. Since NLRP7 is from the same family, we hypothesized that it may form an inflammasome to activate caspase-1.

In order to test this hypothesis, co-localization experiments were performed. Here the co-localization of EGFP fused NLRP7 protein and RFP fused ASC and/or CFP fused Caspase-1 proteins were observed in HEK293FT cells (Figure 5.14). These experiments showed that NLRP7 co-localizes with ASC in more than 90% of ASC specks. On the other hand NLRP7 and Caspase-1 were both nicely dispersed through the cytoplasm in double co-transfections. However in the case of NLRP7, ASC and caspase-1 triple co-transfections, when NLRP7 and ASC were still perfectly (above 90%) co-localizing, caspase-1 was co-localizing with most of these but not all. To see if these proteins also physically interact co-immunoprecipitation experiments were performed. Co-IP experiments showed that caspase-1 (Figure 5.15), ASC (Figure 5.17) and also caspase-5 (Figure 5.16) could interact with NLRP7 in overexpression conditions in HEK293FT cells. By another overexpression experiment, inflammasome activation was tested. For this purpose ASC, pro-caspase-1 and pro-IL-1β plasmids were co-transfected with NLRP7 into HEK293FT cells and inflammasome activation was detected by Western Blotting for mature IL-1β (Figure 5.18). Therefore, it is possible to conclude that NLRP7 is able to form an inflammasome that can activate caspase-1 leading to pro-IL-1β cleavage. In fact, a recent paper that was published while this thesis was being prepared showed clearly that in overexpression conditions NLRP7 is able to form an inflammasome containing ASC and caspase-1 resulting in caspase-1 activation and pro-IL-1β maturation (Khare *et al.*, 2012).

Interestingly, NLRP7 is expressed in immune privilege areas in the body, such as brain, testis and placenta. Also, several NLRP7 mutations were found to be responsible for recurrent hydatidiform moles causing spontaneous abortions. Besides that, for successful development inside the uterus, the embryo has to be implanted to the decidua properly. It is known that secretion profiles of certain cytokines such as LIF, IL-6 and gp130 are crucial for effective implantation of the embryo to the uterus wall (Abrahams, 2011, Makrigiannakis *et al.*, 2011). Thus, the aim of this project was to elucidate whether NLRP7 has a role in immune privilege.

For this purpose, HEC-1-A cells were selected for their endogenous NLRP7 expression. Loss of function experiments could reveal NLRP7's possible role in the pro-

cess of immune privilege. One of the common features of immune privilege areas is an increase in death ligand expression, so that immune cells can be killed and unwanted immune responses can be stopped. This strategy is used by cancer cells as well to escape from the immune system. Here, cDNA levels of several death receptors and ligands were measured by quantitative real time PCR after stable NLRP7 knock-down using shRNA plasmids in HEC-1-A cells. We found that TRAIL-R3, TNF-R2 and TWEAK levels significantly decreased, whereas Fas levels increased upon NLRP7 knock-down (Figure 5.22) which was also confirmed with the FACS data (Figure 5.23a). TRAIL-R3, TNF-R2 and TWEAK surface expression changes could not be confirmed at the protein level using FACS. This may be due to unsuccessful labeling of the expired antibodies. Additionally, p53 and IL-1β were reduced significantly at the mRNA level as well (Figure 5.22).

TRAIL-R3 (DcR1) is a membrane bound decoy death receptor that is totally devoid of a cytoplasmic death domain. This prevents TRAIL-R3 from relaying the apoptotic signals to the cell. Because it competes with other TRAIL receptors DR4 and DR5 for binding to TRAIL it rescues cells from apoptosis, so it is referred to as anti-apoptotic decoy receptor (Sheikh *et al.*, 1999). According to a recent paper another fact is that in recurrent miscarriages TRAIL levels were found to increase (Agostinis *et al.*, 2012). If the data obtained is combined with this literature knowledge, a model can be constructed: Wild type NLRP7 levels stabilize TRAIL-R3 at 'normal' levels, however when there is less functional NLRP7, TRAIL-R3 levels will be reduced (according to real time PCR data) leading to less competition for TRAIL binding and causing much more apoptosis. This may account for the recurrent abortions of women with mutant NLRP7.

Another characteristic feature of immune privilege areas is changes in MHC Class I molecules. In human MHC Class I molecules are expressed by all nucleated cells and while normal tissues express HLA A, B and C, immune privilege sites shift their HLA expression to HLA E and HLA G and they reduce the HLA expression to present less antigens to the immune system. Thus, HLA levels were measured in stable NLRP7 knock-down HEC-1-A cell line using FACS and it was found that HLA A, B, C levels decreased in response to NLRP7 knock-down in comparison to scrambled transfected

control, whereas HLA E and HLA G levels did not change (Figure 5.24). This experiment should be repeated with other cell types, so that effect of NLRP7 on HLA expression can be deduced.

Finally in order to have more insight into the function of NLRP7, its cellular localization was analyzed by making use of an EGFP-NLRP7 fusion protein. This was co-transfected with certain organelle markers and the frequency of co-localization was calculated by counting the number of cells from the different areas of the same sample observed under confocal microscope. Although NLRs can localize in the mitochondria (Tattoli *et al.*, 2008), only 25% of NLRP7 was found to colocalize with mitochondria (Figure 5.13). From these data it is concluded that NLRP7 is a cytoplasmic protein.

In the light of all the experiments and previous literature knowledge, it can be proposed that NLRP7 may have a dual role, namely regulation of both pro-IL-1β synthesis and maturation into IL-1β by the inflammasome structure it forms (Figure 6.1). Besides these, p53 may be responsible for changes in all the death receptors and ligands since it is able to regulate many genes at the transcriptional level.

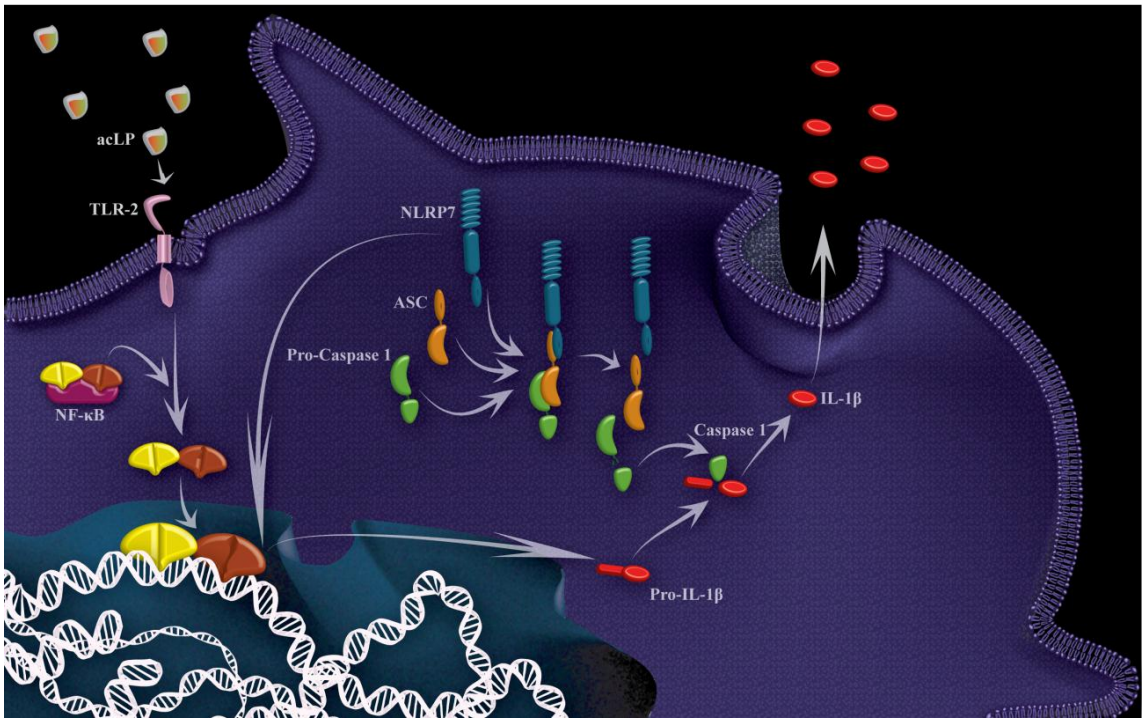

Figure 6.1. Proposed model for the function of NLRP7 in inflammation.

REFERENCES

Abrahams, V.M., 2011, "The Role of the Nod-Like Receptor Family in Trophoblast Innate Immune Responses", *Journal Of Reproductive Immunology*, Vol. 88, No. 2, pp 112-117.

Agostinis, C., R. Bulla, V. Tisato, F. De Seta, S. Alberico, P. Secchiero and G. Zauli, 2012, "Soluble Trail Is Elevated in Recurrent Miscarriage and Inhibits the in Vitro Adhesion and Migration of Htr8 Trophoblastic Cells", *Human Reproduction*, Vol. 27, No. 10, pp 2941-2947.

Akira, S., 2009, "Pathogen Recognition by Innate Immunity and Its Signaling", *Proceedings Of The Japan Academy. Series B, Physical And Biological Sciences*, Vol. 85, No. 4, pp 143-156.

Akira, S., S. Uematsu and O. Takeuchi, 2006, "Pathogen Recognition and Innate Immunity", *Cell*, Vol. 124, No. 4, pp 783-801.

Barker, C.F. and R.E. Billingham, 1977, "Immunologically Privileged Sites", *Advances In Immunology*, Vol. 25, No. 1-54.

Bellgrau, D., D. Gold, H. Selawry, J. Moore, A. Franzusoff and R.C. Duke, 1995, "A Role for Cd95 Ligand in Preventing Graft Rejection", *Nature*, Vol. 377, No. 6550, pp 630-632.

Bennett, M.W., J. O'Connell, C. O'Sullivan G, D. Roche, C. Brady, J. Kelly, J.K. Collins and F. Shanahan, 1999, "Expression of Fas Ligand by Human Gastric Adenocarcinomas: A Potential Mechanism of Immune Escape in Stomach Cancer", *Gut*, Vol. 44, No. 2, pp 156-162.

Bruey, J.M., N. Bruey-Sedano, R. Newman, S. Chandler, C. Stehlik and J.C. Reed, 2004, "Pan1/Nalp2/Pypaf2, an Inducible Inflammatory Mediator That Regulates

Nf-Kappab and Caspase-1 Activation in Macrophages", *The Journal Of Biological Chemistry*, Vol. 279, No. 50, pp 51897-51907.

Chen, G., M.H. Shaw, Y.G. Kim and G. Nunez, 2009, "Nod-Like Receptors: Role in Innate Immunity and Inflammatory Disease", *Annual Review Of Pathology*, Vol. 4, No. 365-398.

Conti, B.J., B.K. Davis, J. Zhang, W. O'Connor, Jr., K.L. Williams and J.P. Ting, 2005, "Caterpiller 16.2 (Clr16.2), a Novel Nbd/Lrr Family Member That Negatively Regulates T Cell Function", *The Journal Of Biological Chemistry*, Vol. 280, No. 18, pp 18375-18385.

Dangl, J.L. and J.D. Jones, 2001, "Plant Pathogens and Integrated Defence Responses to Infection", *Nature*, Vol. 411, No. 6839, pp 826-833.

Ditzian-Kadanoff, R., 1999, "Testicular-Associated Immune Deviation and Prevention of Adjuvant-Induced Arthritis by Three Tolerization Methods", *Scandinavian Journal Of Immunology*, Vol. 50, No. 2, pp 150-158.

Fallarino, F., U. Grohmann, C. Vacca, R. Bianchi, C. Orabona, A. Spreca, M.C. Fioretti and P. Puccetti, 2002, "T Cell Apoptosis by Tryptophan Catabolism", *Cell Death And Differentiation*, Vol. 9, No. 10, pp 1069-1077.

Fiorentino, L., C. Stehlik, V. Oliveira, M.E. Ariza, A. Godzik and J.C. Reed, 2002, "A Novel Paad-Containing Protein That Modulates Nf-Kappa B Induction by Cytokines Tumor Necrosis Factor-Alpha and Interleukin-1beta", *The Journal Of Biological Chemistry*, Vol. 277, No. 38, pp 35333-35340.

Fiszer, D., M. Ulbrecht, N. Fernandez, J.P. Johnson, E.H. Weiss and M. Kurpisz, 1997, "Analysis of Hla Class Ib Gene Expression in Male Gametogenic Cells", *European Journal Of Immunology*, Vol. 27, No. 7, pp 1691-1695.

Franchi, L., R. Munoz-Planillo and G. Nunez, 2012, "Sensing and Reacting to Microbes through the Inflammasomes", *Nature Immunology*, Vol. 13, No. 4, pp 325-332.

Gao, Y., J.M. Herndon, H. Zhang, T.S. Griffith and T.A. Ferguson, 1998, "Antiinflammatory Effects of Cd95 Ligand (Fasl)-Induced Apoptosis", *The Journal Of Experimental Medicine*, Vol. 188, No. 5, pp 887-896.

Girardin, S.E., I.G. Boneca, L.A. Carneiro, A. Antignac, M. Jehanno, J. Viala, K. Tedin, M.K. Taha, A. Labigne, U. Zahringer, A.J. Coyle, P.S. DiStefano, J. Bertin, P.J. Sansonetti and D.J. Philpott, 2003a, "Nod1 Detects a Unique Muropeptide from Gram-Negative Bacterial Peptidoglycan", *Science*, Vol. 300, No. 5625, pp 1584-1587.

Girardin, S.E., I.G. Boneca, J. Viala, M. Chamaillard, A. Labigne, G. Thomas, D.J. Philpott and P.J. Sansonetti, 2003b, "Nod2 Is a General Sensor of Peptidoglycan through Muramyl Dipeptide (Mdp) Detection", *The Journal Of Biological Chemistry*, Vol. 278, No. 11, pp 8869-8872.

Girardin, S.E., L.H. Travassos, M. Herve, D. Blanot, I.G. Boneca, D.J. Philpott, P.J. Sansonetti and D. Mengin-Lecreulx, 2003c, "Peptidoglycan Molecular Requirements Allowing Detection by Nod1 and Nod2", *The Journal Of Biological Chemistry*, Vol. 278, No. 43, pp 41702-41708.

Gratas, C., Y. Tohma, E.G. Van Meir, M. Klein, M. Tenan, N. Ishii, O. Tachibana, P. Kleihues and H. Ohgaki, 1997, "Fas Ligand Expression in Glioblastoma Cell Lines and Primary Astrocytic Brain Tumors", *Brain Pathology*, Vol. 7, No. 3, pp 863-869.

Head, J.R., W.B. Neaves and R.E. Billingham, 1983, "Reconsideration of the Lymphatic Drainage of the Rat Testis", *Transplantation*, Vol. 35, No. 1, pp 91-95.

Honig, A., L. Rieger, M. Kapp, M. Sutterlin, J. Dietl and U. Kammerer, 2004, "Indoleamine 2,3-Dioxygenase (Ido) Expression in Invasive Extravillous Trophoblast Supports Role of the Enzyme for Materno-Fetal Tolerance", *Journal Of Reproductive Immunology*, Vol. 61, No. 2, pp 79-86.

Horikawa, M., N.J. Kirkman, K.E. Mayo, S.M. Mulders, J. Zhou, C.A. Bondy, S.Y. Hsu, G.J. King and E.Y. Adashi, 2005, "The Mouse Germ-Cell-Specific Leucine-Rich Repeat Protein Nalp14: A Member of the Nacht Nucleoside Triphosphatase Family", *Biology Of Reproduction*, Vol. 72, No. 4, pp 879-889.

Hulbert, S.H., C.A. Webb, S.M. Smith and Q. Sun, 2001, "Resistance Gene Complexes: Evolution and Utilization", *Annual Review Of Phytopathology*, Vol. 39, No. 285-312.

Igney, F.H. and P.H. Krammer, 2005, "Tumor Counterattack: Fact or Fiction?", *Cancer Immunology, Immunotherapy : CII*, Vol. 54, No. 11, pp 1127-1136.

Inohara, Chamaillard, C. McDonald and G. Nunez, 2005a, "Nod-Lrr Proteins: Role in Host-Microbial Interactions and Inflammatory Disease", *Annual Review Of Biochemistry*, Vol. 74, No. 355-383.

Ismair, M.G., S.R. Vavricka, G.A. Kullak-Ublick, M. Fried, D. Mengin-Lecreulx and S.E. Girardin, 2006, "Hpept1 Selectively Transports Muramyl Dipeptide but Not Nod1-Activating Muramyl Peptides", *Canadian Journal Of Physiology And Pharmacology*, Vol. 84, No. 12, pp 1313-1319.

Janeway, C.A., Jr., 1989, "Approaching the Asymptote? Evolution and Revolution in Immunology", *Cold Spring Harbor Symposia On Quantitative Biology*, Vol. 54 Pt 1, No. 1-13.

Kawai, T. and S. Akira, 2009, "The Roles of Tlrs, Rlrs and Nlrs in Pathogen Recognition", *International Immunology*, Vol. 21, No. 4, pp 317-337.

Khare, S., A. Dorfleutner, N.B. Bryan, C. Yun, A.D. Radian, L. de Almeida, Y. Rojanasakul and C. Stehlik, 2012, "An Nlrp7-Containing Inflammasome Mediates Recognition of Microbial Lipopeptides in Human Macrophages", *Immunity*, Vol. 36, No. 3, pp 464-476.

Kinoshita, T., Y. Wang, M. Hasegawa, R. Imamura and T. Suda, 2005, "Pypaf3, a Pyrin-Containing Apaf-1-Like Protein, Is a Feedback Regulator of Caspase-1-Dependent Interleukin-1beta Secretion", *The Journal Of Biological Chemistry*, Vol. 280, No. 23, pp 21720-21725.

Kou, Y.C., L. Shao, H.H. Peng, R. Rosetta, D. del Gaudio, A.F. Wagner, T.K. Al-Hussaini and I.B. Van den Veyver, 2008, "A Recurrent Intragenic Genomic Duplication, Other Novel Mutations in Nlrp7 and Imprinting Defects in Recurrent Biparental Hydatidiform Moles", *Molecular Human Reproduction*, Vol. 14, No. 1, pp 33-40.

Kudo, Y., C.A. Boyd, I. Spyropoulou, C.W. Redman, O. Takikawa, T. Katsuki, T. Hara, K. Ohama and I.L. Sargent, 2004, "Indoleamine 2,3-Dioxygenase: Distribution and Function in the Developing Human Placenta", *Journal Of Reproductive Immunology*, Vol. 61, No. 2, pp 87-98.

Laing, K.J., M.K. Purcell, J.R. Winton and J.D. Hansen, 2008, "A Genomic View of the Nod-Like Receptor Family in Teleost Fish: Identification of a Novel Nlr Subfamily in Zebrafish", *BMC Evolutionary Biology*, Vol. 8, No. 42.

Lee, G.K., H.J. Park, M. Macleod, P. Chandler, D.H. Munn and A.L. Mellor, 2002, "Tryptophan Deprivation Sensitizes Activated T Cells to Apoptosis Prior to Cell Division", *Immunology*, Vol. 107, No. 4, pp 452-460.

Lemaitre, B., E. Nicolas, L. Michaut, J.M. Reichhart and J.A. Hoffmann, 1996, "The Dorsoventral Regulatory Gene Cassette Spatzle/Toll/Cactus Controls the Potent Antifungal Response in Drosophila Adults", *Cell*, Vol. 86, No. 6, pp 973-983.

Lich, J.D., K.L. Williams, C.B. Moore, J.C. Arthur, B.K. Davis, D.J. Taxman and J.P. Ting, 2007, "Monarch-1 Suppresses Non-Canonical Nf-Kappab Activation and P52-Dependent Chemokine Expression in Monocytes", *Journal of Immunology*, Vol. 178, No. 3, pp 1256-1260.

Makrigiannakis, A., G. Petsas, B. Toth, K. Relakis and U. Jeschke, 2011, "Recent Advances in Understanding Immunology of Reproductive Failure", *Journal Of Reproductive Immunology*, Vol. 90, No. 1, pp 96-104.

Medzhitov, R., 2001, "Toll-Like Receptors and Innate Immunity", *Nature Reviews. Immunology*, Vol. 1, No. 2, pp 135-145.

Medzhitov, R., P. Preston-Hurlburt and C.A. Janeway, Jr., 1997, "A Human Homologue of the Drosophila Toll Protein Signals Activation of Adaptive Immunity", *Nature*, Vol. 388, No. 6640, pp 394-397.

Meinhardt, A. and M.P. Hedger, 2011, "Immunological, Paracrine and Endocrine Aspects of Testicular Immune Privilege", *Molecular And Cellular Endocrinology*, Vol. 335, No. 1, pp 60-68.

Mellor, A.L. and D.H. Munn, 2004, "Ido Expression by Dendritic Cells: Tolerance and Tryptophan Catabolism", *Nature Reviews. Immunology*, Vol. 4, No. 10, pp 762-774.

Messaed, C., E. Akoury, U. Djuric, J. Zeng, M. Saleh, L. Gilbert, M. Seoud, S. Qureshi and R. Slim, 2011, "Nlrp7, a Nucleotide Oligomerization Domain-Like Receptor Protein, Is Required for Normal Cytokine Secretion and Co-Localizes with Golgi and the Microtubule-Organizing Center", *The Journal Of Biological Chemistry*, Vol. 286, No. 50, pp 43313-43323.

Minas, V., A. Rolaki, S.N. Kalantaridou, J. Sidiropoulos, S. Mitrou, G. Petsas, U. Jeschke, E.A. Paraskevaidis, G. Fountzilas, G.P. Chrousos, N. Pavlidis and A. Makrigiannakis, 2007, "Intratumoral Crh Modulates Immuno-Escape of Ovarian Cancer Cells through Fasl Regulation", *British Journal Of Cancer*, Vol. 97, No. 5, pp 637-645.

Mizuno, K., A.F. Clark and J.W. Streilein, 1989, "Anterior Chamber-Associated Immune Deviation Induced by Soluble Antigens", *Investigative Ophthalmology & Visual Science*, Vol. 30, No. 6, pp 1112-1119.

Munn, D.H., E. Shafizadeh, J.T. Attwood, I. Bondarev, A. Pashine and A.L. Mellor, 1999, "Inhibition of T Cell Proliferation by Macrophage Tryptophan Catabolism", *The Journal Of Experimental Medicine*, Vol. 189, No. 9, pp 1363-1372.

Nasr, I.W., Y. Wang, G. Gao, S. Deng, L. Diggs, D.M. Rothstein, G. Tellides, F.G. Lakkis and Z. Dai, 2005, "Testicular Immune Privilege Promotes Transplantation Tolerance by Altering the Balance between Memory and Regulatory T Cells", *Journal of Immunology*, Vol. 174, No. 10, pp 6161-6168.

Niederkorn, J.Y., 2006, "See No Evil, Hear No Evil, Do No Evil: The Lessons of Immune Privilege", *Nature Immunology*, Vol. 7, No. 4, pp 354-359.

Niederkorn, J.Y., J.W. Streilein and M.L. Kripke, 1983, "Promotion of Syngeneic Intraocular Tumor Growth in Mice by Anterior Chamber-Associated Immune Deviation", *Journal Of The National Cancer Institute*, Vol. 71, No. 1, pp 193-199.

O'Connell, J., M.W. Bennett, G.C. O'Sullivan, J.K. Collins and F. Shanahan, 1999, "Resistance to Fas (Apo-1/Cd95)-Mediated Apoptosis and Expression of Fas Ligand in Esophageal Cancer: The Fas Counterattack", *Diseases Of The Esophagus : Official Journal Of The International Society For Diseases Of The Esophagus / I.S.D.E*, Vol. 12, No. 2, pp 83-89.

Ohno, S., T. Kinoshita, Y. Ohno, T. Minamoto, N. Suzuki, M. Inoue and T. Suda, 2008, "Expression of Nlrp7 (Pypaf3, Nalp7) Protein in Endometrial Cancer Tissues", *Anticancer Research*, Vol. 28, No. 4C, pp 2493-2497.

Okada, K., E. Hirota, Y. Mizutani, T. Fujioka, T. Shuin, T. Miki, Y. Nakamura and T. Katagiri, 2004, "Oncogenic Role of Nalp7 in Testicular Seminomas", *Cancer Science*, Vol. 95, No. 12, pp 949-954.

Qian, J., C. Deveault, R. Bagga, X. Xie and R. Slim, 2007, "Women Heterozygous for Nalp7/Nlrp7 Mutations Are at Risk for Reproductive Wastage: Report of Two Novel Mutations", *Human Mutation*, Vol. 28, No. 7, pp 741.

Ratner, A.J., J.L. Aguilar, M. Shchepetov, E.S. Lysenko and J.N. Weiser, 2007, "Nod1 Mediates Cytoplasmic Sensing of Combinations of Extracellular Bacteria", *Cellular Microbiology*, Vol. 9, No. 5, pp 1343-1351.

Ryan, A.F., R.L. Grendell, D.E. Geraghty and T.G. Golos, 2002, "A Soluble Isoform of the Rhesus Monkey Nonclassical Mhc Class I Molecule Mamu-Ag Is Expressed in the Placenta and the Testis", *Journal of Immunology*, Vol. 169, No. 2, pp 673-683.

Schroder, K. and J. Tschopp, 2010, "The Inflammasomes", *Cell*, Vol. 140, No. 6, pp 821-832.

Schwandner, R., R. Dziarski, H. Wesche, M. Rothe and C.J. Kirschning, 1999, "Peptidoglycan- and Lipoteichoic Acid-Induced Cell Activation Is Mediated by Toll-Like Receptor 2", *The Journal Of Biological Chemistry*, Vol. 274, No. 25, pp 17406-17409.

Shaw, M.H., T. Reimer, Y.G. Kim and G. Nunez, 2008, "Nod-Like Receptors (Nlrs): Bona Fide Intracellular Microbial Sensors", *Current Opinion In Immunology*, Vol. 20, No. 4, pp 377-382.

Sheikh, M.S., Y. Huang, E.A. Fernandez-Salas, W.S. El-Deiry, H. Friess, S. Amundson, J. Yin, S.J. Meltzer, N.J. Holbrook and A.J. Fornace, Jr., 1999, "The Antiapoptotic Decoy Receptor Trid/Trail-R3 Is a P53-Regulated DNA Damage-Inducible Gene That Is Overexpressed in Primary Tumors of the Gastrointestinal Tract", *Oncogene*, Vol. 18, No. 28, pp 4153-4159.

Slim, R., R. Bagga, W. Chebaro, R. Srinivasan and N. Agarwal, 2009, "A Strong Founder Effect for Two Nlrp7 Mutations in the Indian Population: An Intriguing Observation", *Clinical Genetics*, Vol. 76, No. 3, pp 292-295.

Slim, R. and A. Mehio, 2007, "The Genetics of Hydatidiform Moles: New Lights on an Ancient Disease", *Clinical Genetics*, Vol. 71, No. 1, pp 25-34.

Sodergren, E., G.M. Weinstock, E.H. Davidson, R.A. Cameron, R.A. Gibbs, R.C. Angerer, L.M. Angerer, M.I. Arnone, D.R. Burgess, R.D. Burke, J.A. Coffman, M. Dean, M.R. Elphick, C.A. Ettensohn, K.R. Foltz, A. Hamdoun, R.O. Hynes, W.H. Klein, W. Marzluff, D.R. McClay, R.L. Morris, A. Mushegian, J.P. Rast, L.C. Smith, M.C. Thorndyke, V.D. Vacquier, G.M. Wessel, G. Wray, L. Zhang, C.G. Elsik, O. Ermolaeva, W. Hlavina, G. Hofmann, P. Kitts, M.J. Landrum, A.J. Mackey, D. Maglott, G. Panopoulou, A.J. Poustka, K. Pruitt, V. Sapojnikov, X. Song, A. Souvorov, V. Solovyev, Z. Wei, C.A. Whittaker, K. Worley, K.J. Durbin, Y. Shen, O. Fedrigo, D. Garfield, R. Haygood, A. Primus, R. Satija, T. Severson, M.L. Gonzalez-Garay, A.R. Jackson, A. Milosavljevic, M. Tong, C.E. Killian, B.T. Livingston, F.H. Wilt, N. Adams, R. Belle, S. Carbonneau, R. Cheung, P. Cormier, B. Cosson, J. Croce, A. Fernandez-Guerra, A.M. Geneviere, M. Goel, H. Kelkar, J. Morales, O. Mulner-Lorillon, A.J. Robertson, J.V. Goldstone, B. Cole, D. Epel, B. Gold, M.E. Hahn, M. Howard-Ashby, M. Scally, J.J. Stegeman, E.L. Allgood, J. Cool, K.M. Judkins, S.S. McCafferty, A.M. Musante, R.A. Obar, A.P. Rawson, B.J. Rossetti, I.R. Gibbons, M.P. Hoffman, A. Leone, S. Istrail, S.C. Materna, M.P. Samanta, V. Stolc, W. Tongprasit, Q. Tu, K.F. Bergeron, B.P. Brandhorst, J. Whittle, K. Berney, D.J. Bottjer, C. Calestani, K. Peterson, E. Chow, Q.A. Yuan, E. Elhaik, D. Graur, J.T. Reese, I. Bosdet, S. Heesun, M.A. Marra, J. Schein, M.K. Anderson, V. Brockton, K.M. Buckley, A.H. Cohen, S.D. Fugmann, T. Hibino, M. Loza-Coll, A.J. Majeske, C. Messier, S.V. Nair, Z. Pancer, D.P. Terwilliger, C. Agca, E. Arboleda, N. Chen, A.M. Churcher, F. Hallbook, G.W. Humphrey, M.M. Idris, T. Kiyama, S. Liang, D. Mellott, X. Mu, G. Murray, R.P. Olinski, F. Raible, M. Rowe, J.S. Taylor, K. Tessmar-Raible, D. Wang, K.H. Wilson, S. Yaguchi, T. Gaasterland, B.E. Galindo, H.J. Gunaratne, C. Juliano, M. Kinukawa, G.W. Moy, A.T. Neill, M. Nomura, M. Raisch, A. Reade, M.M. Roux, J.L. Song, Y.H. Su, I.K. Townley, E. Voronina, J.L. Wong, G. Amore, M. Branno, E.R. Brown, V. Cavalieri, V. Duboc, L. Duloquin, C. Flytzanis, C. Gache, F. Lapraz, T. Lepage, A. Locascio, P. Martinez, G. Matassi, V. Matranga, R. Range, F. Rizzo, E. Rottinger, W.

Beane, C. Bradham, C. Byrum, T. Glenn, S. Hussain, G. Manning, E. Miranda, R. Thomason, K. Walton, A. Wikramanayke, S.Y. Wu, R. Xu, C.T. Brown, L. Chen, R.F. Gray, P.Y. Lee, J. Nam, P. Oliveri, J. Smith, D. Muzny, S. Bell, J. Chacko, A. Cree, S. Curry, C. Davis, H. Dinh, S. Dugan-Rocha, J. Fowler, R. Gill, C. Hamilton, J. Hernandez, S. Hines, J. Hume, L. Jackson, A. Jolivet, C. Kovar, S. Lee, L. Lewis, G. Miner, M. Morgan, L.V. Nazareth, G. Okwuonu, D. Parker, L.L. Pu, R. Thorn and R. Wright, 2006, "The Genome of the Sea Urchin Strongylocentrotus Purpuratus", *Science*, Vol. 314, No. 5801, pp 941-952.

Swaan, P.W., T. Bensman, P.M. Bahadduri, M.W. Hall, A. Sarkar, S. Bao, C.M. Khantwal, S. Ekins and D.L. Knoell, 2008, "Bacterial Peptide Recognition and Immune Activation Facilitated by Human Peptide Transporter Pept2", *American Journal Of Respiratory Cell And Molecular Biology*, Vol. 39, No. 5, pp 536-542.

Tattoli, I., L.A. Carneiro, M. Jehanno, J.G. Magalhaes, Y. Shu, D.J. Philpott, D. Arnoult and S.E. Girardin, 2008, "Nlrx1 Is a Mitochondrial Nod-Like Receptor That Amplifies Nf-Kappab and Jnk Pathways by Inducing Reactive Oxygen Species Production", *EMBO Reports*, Vol. 9, No. 3, pp 293-300.

Ting, J.P., R.C. Lovering, E.S. Alnemri, J. Bertin, J.M. Boss, B.K. Davis, R.A. Flavell, S.E. Girardin, A. Godzik, J.A. Harton, H.M. Hoffman, J.P. Hugot, N. Inohara, A. Mackenzie, L.J. Maltais, G. Nunez, Y. Ogura, L.A. Otten, D. Philpott, J.C. Reed, W. Reith, S. Schreiber, V. Steimle and P.A. Ward, 2008, "The Nlr Gene Family: A Standard Nomenclature", *Immunity*, Vol. 28, No. 3, pp 285-287.

Tong, Z.B., L. Gold, K.E. Pfeifer, H. Dorward, E. Lee, C.A. Bondy, J. Dean and L.M. Nelson, 2000, "Mater, a Maternal Effect Gene Required for Early Embryonic Development in Mice", *Nature Genetics*, Vol. 26, No. 3, pp 267-268.

Wang, C.M., P.H. Dixon, S. Decordova, M.D. Hodges, N.J. Sebire, S. Ozalp, M. Fallahian, A. Sensi, F. Ashrafi, V. Repiska, J. Zhao, Y. Xiang, P.M. Savage, M.J. Seckl and R.A. Fisher, 2009, "Identification of 13 Novel Nlrp7 Mutations in 20 Families with Recurrent Hydatidiform Mole; Missense Mutations Cluster in the

Leucine-Rich Region", *Journal Of Medical Genetics*, Vol. 46, No. 8, pp 569-575.

Wang, Y., M. Hasegawa, R. Imamura, T. Kinoshita, C. Kondo, K. Konaka and T. Suda, 2004, "Pynod, a Novel Apaf-1/Ced4-Like Protein Is an Inhibitor of Asc and Caspase-1", *International Immunology*, Vol. 16, No. 6, pp 777-786.

Whittum, J.A., J.Y. Niederkorn, J.P. McCulley and J.W. Streilein, 1982, "Intracameral Inoculation of Herpes Simplex Virus Type I Induces Anterior Chamber Associated Immune Deviation", *Current Eye Research*, Vol. 2, No. 10, pp 691-697.

Yoneyama, M. and T. Fujita, 2008, "Structural Mechanism of Rna Recognition by the Rig-I-Like Receptors", *Immunity*, Vol. 29, No. 2, pp 178-181.